



**Universiteit
Leiden**
The Netherlands

Bioengineering and biophysics of viral hemorrhagic fever
Tang, H.

Citation

Tang, H. (2023, September 19). *Bioengineering and biophysics of viral hemorrhagic fever*. Retrieved from <https://hdl.handle.net/1887/3641674>

Version: Publisher's Version

License: [Licence agreement concerning inclusion of doctoral thesis in the Institutional Repository of the University of Leiden](#)

Downloaded from: <https://hdl.handle.net/1887/3641674>

Note: To cite this publication please use the final published version (if applicable).

EBOLA VIRUS-LIKE PARTICLES REPROGRAM CELLULAR METABOLISM

Ebola virus can trigger a release of pro-inflammatory cytokines with subsequent vascular leakage and impairment of clotting finally leading to multiorgan failure and shock after entering and infecting patients. Ebola virus is known to directly target endothelial cells and macrophages, even without infecting them, through direct interactions with viral proteins. These interactions affect cellular mechanics and immune processes, which are tightly linked to other key cellular functions such as metabolism. However, research regarding metabolic activity of these cells upon viral exposure remains limited, hampering our understanding of its pathophysiology and progression. Therefore, in the present study, an untargeted cellular metabolomic approach was performed to investigate the metabolic alterations of primary human endothelial cells and M1 and M2 macrophages upon exposure to Ebola virus-like particles (VLP). The results show that Ebola VLP led to metabolic changes among endothelial, M1, and M2 cells. Differential metabolite abundance and perturbed signaling pathway analysis further identified specific metabolic features, mainly in fatty acid-, steroid-, and amino acid-related metabolism pathways for all the three cell types, in a host cell specific manner. Taken together, this work characterized for the first time the metabolic alternations of endothelial cells and two primary human macrophage subtypes after Ebola VLP exposure, and identified the potential metabolites and pathways differentially affected, highlighting the important role of those host cells in disease development and progression.

Huaqi Tang, Yasmine Abouleila, Anno Saris, Yoshihiro Shimizu, Tom H.M. Ottenhoff, Alireza Mashaghi. *Journal of Molecular Medicine* 2023.

<https://doi.org/10.1007/s00109-023-02309-4>

1 Introduction

The outbreak of Ebola in West and Equatorial Africa has heightened worldwide concern. Ebola virus (EBOV) is a negative-sense, single-stranded, enveloped RNA virus that belongs to the Filoviridae family and etiological agent of a critical, often lethal disease known as Ebola hemorrhagic fever (HF) [1, 2]. The hemorrhagic disease caused by EBOV is characterized by initial fever and malaise followed by gastrointestinal symptoms, bleeding, shock, and multiorgan failure with case fatality rates ranging from 25 to 90% [1-3]. The recent Ebola outbreak (2018–2020) in the Democratic Republic of the Congo has claimed 2299 lives and the number of cases exceeded 3300, making it second only to the largest Ebola epidemic in West Africa of 2014–2016, highlighting the continued re-emergence of this pathogen [4]. Even though the first recorded outbreak was in 1976, much of the pathogenesis of EBOV remains unclear.

Macrophages are known as early targets and play an important role in EBOV pathogenesis [5, 6]. Infection of macrophages by EBOV stimulates the abnormal production of proinflammatory and immunomodulatory cytokines and chemokines (cytokine storm), disrupting vascular permeability, and recruitment of additional susceptible cells to the site of infection, which facilitates the systemic dissemination of the virus and leads to the development of viral hemorrhagic fever syndrome [5, 7, 8]. Moreover, secreted viral proteins do alter the balance between pro- and anti-inflammatory cytokines produced by non-infected macrophage cells upon exposure [7]. This effect on non-infected macrophages together with other immune cells can facilitate viral dissemination, establish systemic inflammation, and trigger an excessive cytokine storm that is detrimental for survival [6, 7]. Noninfectious virus-like particles (VLP) expressing EBOV glycoproteins (GPs) and matrix proteins were found to significantly regulate the gene expression profiles of primary human macrophages [9]. However, macrophages are phenotypically heterogeneous depending upon the type of challenge encountered and accordingly perform disparate functions in the human body that may impact the outcome of the host immune responses. The cells show

significant plasticity and metabolic reprogramming has been reported for macrophages in various pathological conditions. Macrophages are generally skewed towards two polarization subtypes, namely M1 or classically activated macrophages, which are elicited by exposure to proinflammatory signals, associate with production of proinflammatory cytokines (IL-1 β , IL-6, IL-12, IL-23, TNF- α , etc.), support Th1 cell immunity [10], and mediate clearance of pathogens [11]; and M2 or alternatively activated macrophages, which are anti-inflammatory and immunoregulatory macrophages, secrete high amounts of anti-inflammatory cytokines (IL-4, IL-10, TGF- β , etc.) to promote resolution of inflammation, contribute to wound healing, support Treg activation [12], and retain homeostasis [13, 14]. Considering the importance of macrophages as major initial targets of EBOV, the different polarization status of macrophages might well influence EBOV pathogenesis.

Vascular instability and dysregulation are hallmarks of the pathogenesis in Ebola HF [15, 16]. It is thought that endothelial dysfunction can be caused either by proinflammatory cytokines (e.g., TNF- α) released from EBOV-infected monocytes/macrophages, or directly following EBOV infection of endothelial cells (ECs) [17]. Additionally, EBOV GPs are regarded as crucial determinants in the induction of cytotoxicity and injury in ECs, and consequently contribute to vascular dysregulation [6, 17-21]. Mechanical disruption of endothelial layers has been directly linked to the Rho/ROCK pathway, and can be reversed by Rho/ROCK inhibitors [18]. However, whether the pathology is limited to mechanics or also involves metabolic reprogramming is not known. The link between mechanics and metabolism has been widely recognized [22]. However, there is limited understanding of endothelial dysfunction that develops during EBOV pathogenesis, in particular, studies that characterize the virally induced metabolites changes in ECs are scarce.

Recent studies showcase that viral pathogenesis is significantly associated with hijacking host metabolic systems [23]. Thus, exploiting altered host metabolism and metabolic pathways represents a new research avenue for understanding the pathogenic mechanisms and will provide new insights on key checkpoints for biomarker discovery as well as novel

drug targets for therapy. Metabolites represent the end products of biochemical pathways and therefore provide the most downstream biological/phenotypic knowledge. Recently, metabolomics proved expedient in aiding in the efforts to understand virus-host interactions as it is capable of providing a direct snapshot of the host metabolic profile in response to infection [24-27]. Particular cellular metabolic pathways such as carbohydrate, fatty acid, and nucleotide metabolism, have been reported to be altered as a result to infection by different viruses [28]. Most likely, each viral species triggers unique host metabolic alterations [24]. As such, various host metabolic reprogramming is associated with Influenza virus [29], Adenovirus [30], Dengue virus [31], Zika virus [32], Enterovirus [28] and SARS-CoV-2 [33]. Yet, very little is known about host metabolic reprogramming as a result to EBOV.

Investigations regarding the metabolic alterations to ECs and macrophages triggered by EBOV are limited. To address this critical gap in knowledge, we studied the impact of Ebola VLP on ECs and the different polarization status of macrophages by untargeted cellular metabolomics using direct infusion-mass spectrometry (DI-MS). Here, we dissect the intracellular metabolite alternations of ECs and M1/M2 macrophages treated by Ebola VLP and show that Ebola VLP can trigger changes mainly in fatty acid-, steroid-, and amino acid-related metabolism pathways for the three cell types, in a cell specific manner. This study demonstrates the strength of metabolomics for biomarker discovery and elucidates the effect of virus on host cells.

2 Materials and Methods

2.1 Cell culture

Primary human umbilical vein endothelial cells (HUVECs) were provided by Leiden University Medical Center. HUVECs were cultured in Endothelial Cell Basal Medium 2 (C-22211; PromoCell) supplemented with Endothelial Cell Growth Medium 2 SupplementMix

(C-39216; PromoCell) and 1% penicillin–streptomycin under 5% CO₂, 37 °C incubator. HUVECs between passages 3 and 4 were used in all experiments.

Peripheral blood mononuclear cells (PBMCs) were isolated from buffy coats of healthy blood bank donors after informed consent was provided. This study was approved by Sanquin' ethical advisory board and in accordance with the declaration of Helsinki and according to Dutch legislation. Monocytes were isolated through density gradient centrifugation over Ficoll-Paque followed by magnetic-activated cell sorting (MACS) using CD14 microbeads (130–097-052, Miltenyi Biotec) and differentiated into M1 or M2 macrophages with 5 ng/ml of granulocyte–macrophage colony-stimulating factor (GM-CSF; 130–093-864, Miltenyi Biotec) or 50 ng/ml macrophage colony-stimulating factor (M-CSF; 130–096-489, Miltenyi Biotec), respectively [10]. Cells were cultured at 37 °C/5% CO₂ in RPMI 1640 medium (31,870,025, Gibco) supplemented with 10% FBS, 2 mM L-alanyl-L-glutamine (GlutaMAX; 35050038, Gibco), and penicillin–streptomycin (35050038, Gibco). As quality control, macrophages were stained for surface expression of CD14, CD163, and CD11b acquired on a flow cytometry (BD LSRFortessa, BD Biosciences). Macrophage differentiation and activation status was determined by quantifying IL-12 and IL-10 secretion by ELISA following stimulation of cells in the presence of 100 ng/ml lipopolysaccharide (LPS) for 24 h [14] (**Figure S1**).

2.2 Sample preparation for Mass Spectrometry

ECs and M1/M2 macrophages were seeded in 6-well plates at a density of 0.9×10^6 cells/well and either treated with 1 µg/ml Ebola VLP (ZEBOVLP-100, The Native Antigen Company) or Ebola VLP buffer only as control (400 mM NaCl, 20 mM Tris–HCl pH8, 10 mM sodium citrate). At 2 h post-treatment, which was based on our previous study and other literature [9, 18], cells were washed with 3 × PBS then ice-cold 0.7% NaCl and subsequently lysed by ice-cold 80% methanol. Lysates mixture was sonicated for 10 min at room temperature before centrifugation at 16,000 rcf for 10 min at 4 °C, after which the supernatants were extracted with twice liquid–liquid extraction procedure using ice-cold

water/methanol/chloroform (1/1/1, v/v/v). The methanol/water (aqueous) phase and chloroform (organic) phase were evaporated separately and dried materials were stored at $-80\text{ }^{\circ}\text{C}$ for subsequent DI-MS analysis.

2.3 Mass spectrometry

Prior to mass spectrometry (MS) measurements, dried extracts were reconstituted in $25\text{ }\mu\text{L}$ of 50% MeOH and 2 mM ammonium formate buffer for the aqueous phase, while for the organic phase, extracts were reconstituted in 80% acetonitrile and 2 mM ammonium formate buffer. From each sample condition, aliquot of $2\text{ }\mu\text{L}$ was added to a platinum-coated glass capillary with $2\text{--}3\text{ }\mu\text{m}$ bore size (CT-1, Humanix). All reagents used in the ionization solvents were of LC-MS grade and were obtained from Sigma-Aldrich. The capillary containing the aliquot was then attached to a nanoelectrospray adapter (nano-ESI) that is connected to the Q-Exactive mass spectrometer (Thermo Fisher Scientific) used in the analysis equipped with a nanospray source (Nanospray Flex; Thermo Fisher Scientific) for subsequent analysis. The mass spectrometer used was previously calibrated using Pierce LTQ Velos ESI calibration solution (Thermo Fisher Scientific). Measurements were performed in positive ion mode. The distance between the capillary and the inlet of the instrument was set to 2 mm and the inlet capillary temperature was set to $200\text{ }^{\circ}\text{C}$. The spray voltage was chosen to be 1.5 kV, maintaining a spray current between 100 and 150 nA. The resolution was set to 120,000 full width half-maximum. For untargeted analysis, selected ion monitoring (SIM) mode was chosen, scanning from a range of 100 to 1000 m/z with increments of 20 m/z. This method ensures a higher dynamic range in addition to a low signal to noise ratios without giving in on mass accuracy, thus enhancing the number of detected metabolites [34].

2.4 Data preprocessing

Data generated from the mass spectrometry measurements was transformed from Thermo Fisher Scientific's raw proprietary format to.txt files containing centroided m/z peaks using

an in-house script. The converted data was then imported to R statistical software to assess the data and to perform quality control checks. Peak alignment was done using Sciex MarkerView software and the aligned data was further processed in R. A mass defect filter [35] was applied to remove salt clusters and artefacts from the dataset. Next, peaks with signal to noise ratio (S/N) < 3 were removed. Subsequently, a blank and medium subtraction filter was applied to remove background peaks. Finally, data was normalized using log₂ transformation and scaled using pareto-scale. The dataset was then divided into three groups: ECs treated and untreated with Ebola VLP, M1 macrophages treated and untreated with Ebola VLP, and M2 macrophages treated and untreated with Ebola VLP.

2.5 Statistical analysis

To demonstrate the metabolic profiles across the different samples in a reduced dimensional space, a principal component analysis (PCA) and a partial least squares discriminant analysis (PLS-DA) were carried out using the R statistical software. PCA aims to reduce dimensionality linearly and creates a new set of vectors that maximize the variance explained, while a PLS-DA tries to discriminate between groups by maximizing the covariance among a specific outcome and a matrix of metabolites [36, 37]. PCA was performed with the `prcomp` function from the `basic stats` package in R. PLS-DA was carried out with the `mixOmics` package in R. After normality check, data was split into parametric and non-parametric sub datasets. To discern the difference in the metabolic profile done due to Ebola VLP, univariate analysis, namely, Welch's *t*-test (on the parametric portion of the data) and Wilcoxon rank-sum test (on the non-parametric portion of the data), were carried out and results were visualized using a volcano plot. Peaks with more than 1 log₂ fold change or less than -1 log₂ fold change and with an FDR-corrected *p*-value < 0.1 were selected as significant and visualized with a heatmap. For peak identification, the significant peaks were run through an in-house script that matches the peaks against different metabolic databases, i.e., Kyoto Encyclopedia of Genes and Genomics (KEGG, <https://www.genome.jp/kegg/>), Human Metabolome Database (HMDB, <https://hmdb.ca/>),

and Lipid maps structure database (LMSD, <https://www.lipidmaps.org/>). This tool uses pathway topological analysis accounting for the impact of individual detected metabolites within a pathway. The analysis depends on the pathway structure and the position of a metabolite within a pathway, meaning that central or nodal positions of metabolites in a pathway will have a greater impact than marginal or isolated positions.

3 Results

3.1 Global metabolic changes in ECs/M1/M2 following Ebola VLP treatment

To assess the possible metabolic alterations induced in ECs, M1, and M2 upon treatment with Ebola VLP, metabolomics data from samples were subjected to an unsupervised PCA followed by a supervised PLS-DA for visualization in a reduced dimensional space. The PCA plots show well-clustering behavior for both ECs and M2 groups (**Figure 1A and C; Figure S2**). However, M1 groups show a degree of overlapping as shown in **Figure 1B**, which may indicate a similarity in the metabolic profile between the two conditions. Then, a supervised PLS-DA was performed and derived score plot revealed a clear clustering behavior (**Figure 1D, E and F**), with specific metabolic profiles for each condition, in all the three groups. Next, Welch's *t*-test and Wilcoxon rank-sum test were performed to narrow down peaks that are significantly different between the Ebola VLP treated and untreated conditions in each group. The distribution of significant and insignificant peaks can be visualized in the volcano plot (**Figure S3**). Furthermore, a heatmap was created to visualize only the intensities of respective significant peaks with FDR-corrected *p*-value < 0.1 in every sample (**Figure 2**). These visualized results provide an overview of the metabolic alternations in the three cell groups after Ebola VLP treatment; however, a more detailed analysis is necessary to better understand how Ebola affects cellular metabolism.

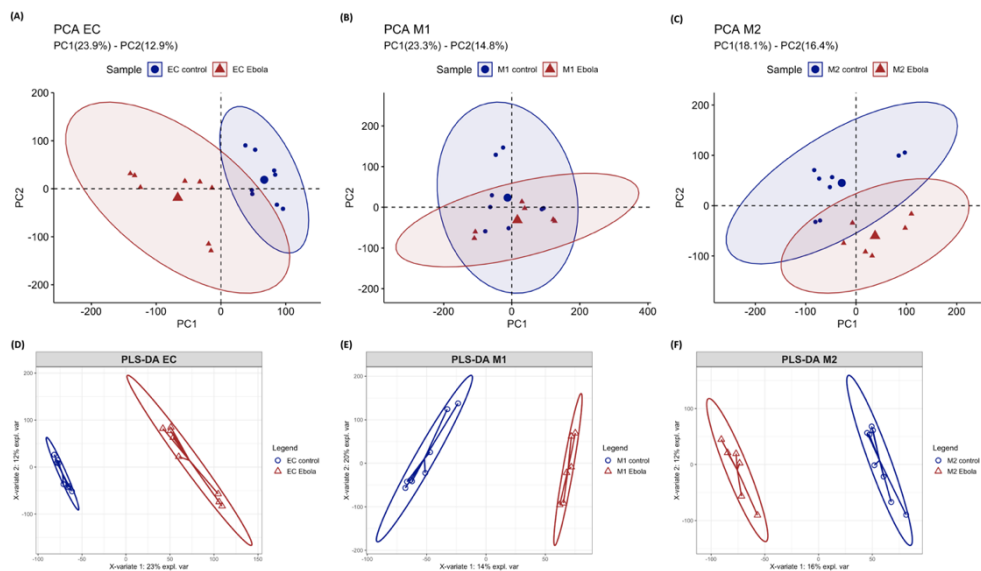


Figure 1. Principal component analysis and partial least squares discriminant analysis of ECs, M1, and M2 after treatment with/without Ebola VLP. The differences in the metabolic profiles between Ebola VLP treated vs. untreated ECs, M1, and M2 are shown in PCA (A, B, C) and PLS-DA (D, E, F), respectively. In both PCA and PLS-DA, red triangles represent cells cultured in the presence of Ebola VLP; blue circles are cells cultured without. Each triangle/circle corresponds to a sample.

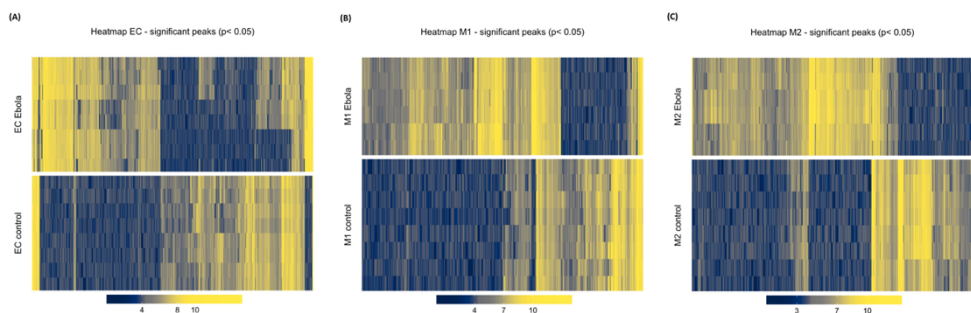


Figure 2. Heatmap of respective significant peaks found in ECs, M1, and M2 after treatment with Ebola VLP in comparison with untreated. Heatmap visualizing the intensity

of each significant peak measured in ECs (A), M1 (B), and M2 (C). The color scales between dark blue and bright yellow represent lower intensity to higher intensity, respectively.

3.2 Potentially altered metabolites and metabolic pathways in Ebola VLP-treated cells

To identify altered metabolites in response to Ebola VLP, the exact masses of the significant peaks resulted from the *t*-test were matched against databases, as mentioned in detail in the “Statistical analysis” section. A level 4 identification confidence could be reached to get unequivocal chemical formulas using the spectral information (e.g., adduct, isotope) [38-40]. Among the statistically significant peaks found, potential matches were identified. A summary of the putatively identified metabolites and lipids in ECs, M1, and M2 with *p*-value, adjusted *p*-value, chemical formula, class, and possible metabolic pathway for each compound is shown in **Table S1-S12**, respectively. A color map for visualizing the distribution of lipid classes is shown in **Figure 3**.

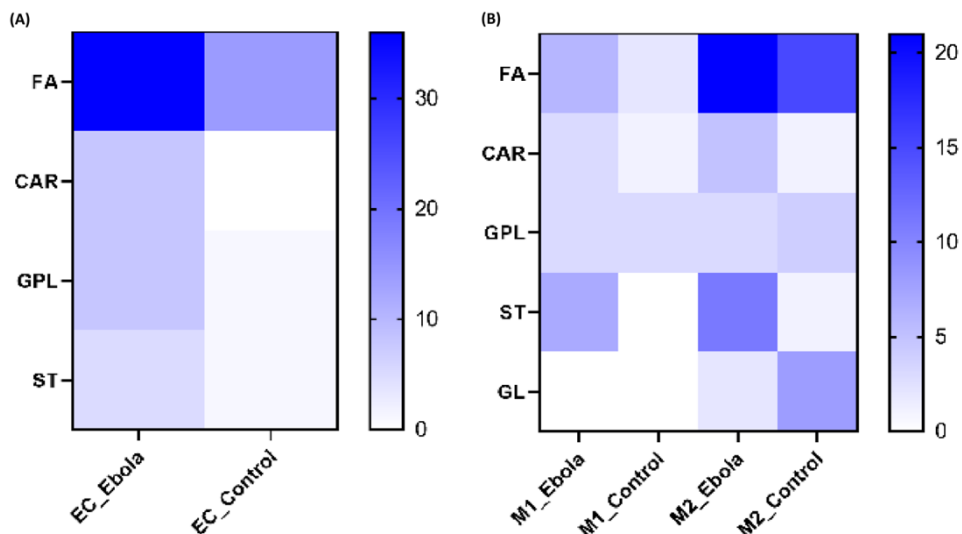


Figure 3. Distribution of lipid classes across ECs, M1, and M2 after treatment with Ebola VLP compared to control. The distributions of several lipid classes, namely, FA, CAR, GPL,

ST, and GL for treated cells compared to their control, are shown in (A) and (B), respectively. GL was detectable in M2 only. The number of peaks matched in the database was counted; each hit corresponds to one peak encountered once. All peaks were filtered to abbreviation: CAR, acylcarnitine; FA, fatty acids; GL, glycerolipids; GPL, glycerophospholipids; ST, sterol lipids.

To gain further insight in the potential metabolic disruptions of Ebola VLP-treated cells, a pathway analysis was performed with respect to the significantly changed metabolites. A total of 7 pathways were observed to be potentially regulated in Ebola VLP-treated ECs, namely biosynthesis of unsaturated fatty acids, linoleic acid metabolism, arachidonic acid metabolism, glycerophospholipid metabolism, primary bile acid biosynthesis, glyoxylate and dicarboxylate metabolism, and valine, leucine, and isoleucine degradation. Meanwhile, alanine, aspartate and glutamate metabolism, arginine biosynthesis, histidine metabolism, glutamine and glutamate metabolism, glutathione metabolism, arginine and proline metabolism, purine metabolism, and pyrimidine metabolism pathways were observed in ECs without treatment (**Table 1**).

Similarly, the pathway analysis was also performed on M1 and M2 macrophages. The butanoate metabolism, pantothenate and CoA biosynthesis, ubiquinone and other terpenoid-quinone biosynthesis, steroid hormone biosynthesis, steroid degradation, and cysteine and methionine metabolism pathways were found modulated in M1 after Ebola VLP treatment, while the fatty acid degradation pathway was more evident in the M1 control group. Through the pathway analysis, we also confirmed a modulation of arginine and proline metabolism; pentose phosphate pathway; valine, leucine, and isoleucine biosynthesis; arachidonic acid metabolism; steroid hormone biosynthesis; primary and secondary bile acid biosynthesis; pentose and glucuronate interconversions; linoleic acid metabolism; biosynthesis of unsaturated fatty acids; retinol metabolism; tryptophan metabolism; and glycerophospholipid metabolism in the M2 Ebola VLP-treated group.

Meanwhile, steroid hormone biosynthesis; arginine and proline metabolism; alanine, aspartate, and glutamate metabolism; valine, leucine, and isoleucine degradation; cholesterol biosynthetic pathway; steroid biosynthesis; ether lipid metabolism; glycerophospholipid metabolism; linoleic acid metabolism; alpha-linolenic acid metabolism; arachidonic acid metabolism; and sphingolipid metabolism were found more prominent in the M2 untreated group (for details, refer to the **Table S1-S12**).

Table 1. Distinct metabolite signatures in ECs, M1, and M2 after Ebola VLP treatment

Samples	Pathway	Hits	Metabolites
ECs_Ebola	Biosynthesis of unsaturated fatty acids	2	FA 20:4 (Arachidonic acid), FA 22:0 (Docosanoic acid)
	Linoleic acid metabolism	5	FA 18:2 (Linoleic acid), FA 20:4 (Arachidonic acid), FA 18:2:O, FA 18:2:O3 (9,12,13, TriHODE), PC O-42:4 (Lecithin)
	Arachidonic acid metabolism	3	FA 20:0:O (Thromboxane), FA 20:4 (Arachidonic acid), PC O-42:4 (Lecithin)
	Glycerophospholipid metabolism	1	PC O-42:4 (Lecithin)
	Bile acid biosynthesis	1	ST 27:1;O3
	Valine, leucine, isoleucine degradation	1	FA 5:1;O
	Lysine degradation	1	FA 5:1;O
	alpha-Linolenic acid metabolism	3	FA 9:1;O, FA 18:3:O, PC O-42:4 (Lecithin)
	Phospholipid metabolism	1	CDP-DG 25:0
	Valine, leucine and isoleucine biosynthesis	1	FA 5:1;O
	Pantothenate and CoA biosynthesis	1	FA 5:1;O
	Fatty acid biosynthesis	5	FA 10:0, FA 10:1;O, FA 12:1, FA 12:1:O, FA 16:1;O
	Fatty acid degradation	1	FAL 16:0
	Steroid hormone biosynthesis	1	ST 21:3;O2 (Progesterone)
	Alanine, aspartate and glutamate metabolism	2	L-Aspartic acid, L-Glutamic acid
ECs_Control	Arginine biosynthesis	2	L-Aspartic acid, L-Glutamic acid
	Histidine metabolism	2	L-Aspartic acid, L-Glutamic acid
	Glutamine and glutamate metabolism	1	L-Glutamic acid
	Glutathione metabolism	4	L-Glutamic acid, gamma-Glutamylvaline, Glutamyllysine, Glutathione
	Arginine and proline metabolism	1	L-4-Hydroxyglutamate semialdehyde
	Purine metabolism	3	Deoxyadenosine monophosphate (DAMP), N-Acetylneuraminic acid, N-Acetyl-a-neuraminic acid, 2'-Deoxyguanosine 5'-monophosphate, Adenosine 2'-phosphate (AMP), 2-hydroxy-dAMP, Adenosine 3',5'-diphosphate, dGDP, ADP
	Pyrimidine metabolism	1	Dihydrothymine
	Butanoate metabolism	1	FA 5:1;O2
	Pantothenate and CoA biosynthesis	1	FA 5:1;O2
	Ubiquinone and other terpenoid-quinone biosynthesis	2	2-Polyprenyl-6-methoxyphenol, Ubiquinol

M1_Control	Steroid hormone biosynthesis	2	ST 19:2;O2, ST 19:3;O2
	Steroid degradation	2	ST 19:2;O2, ST 19:3;O2
	Cysteine and methionine metabolism	1	3-methyl-thiopropionic acid
	Glycerophospholipid metabolism	1	LPC 18:0
	Citrate acid cycle	1	Oxoglutaric acid
	Fatty acid degradation	1	CAR 16:0 (L-palmitoyl/carnitine)
	Arginine and proline metabolism	1	L-Proline
	Pentose phosphate pathway	1	Deoxyribose
	Valine, leucine and isoleucine biosynthesis	2	FA 5:0;O2, Isopropylmaleic acid
	Pantothenate and CoA biosynthesis	1	FA 5:0;O2
M2_Ebola	Arachidonic acid metabolism	5	Tetranor 12-HETE, FA 20:5;O, FA 20:4;O, FA 20:3;O (15(S)-Hydroxyicosatrienoic acid), FA 20:0;O (Thromboxane)
	Steroid hormone biosynthesis	7	ST 19:2;O2, ST 19:1;O2, ST 19:0;O2, ST 19:3;O2 (Androstenedione), ST 19:2;O3 (17beta,19-dihydroxyandrost-4-en-3-one), ST 19:4;O3, ST 18:3;O2(Estradiol)
	Primary and Secondary bile acid biosynthesis	1	ST 24:1;O4
	Pentose and glucuronate interconversions	1	Cholesterol glucuronide
	Linoleic acid metabolism	1	FA 18:2 (linoleic acid)
	Biosynthesis of unsaturated fatty acids	3	FA 18:2 (linoleic acid), FA 20:5 (EPA), FA 22:0 (Behenic acid)
	Retinol metabolism	1	Retinoic Acid
	Tryptophan metabolism	1	5-Hydroxyindoleacetyl/glycine
	Glycerophospholipid metabolism	1	LPC 20:4 (2-Lysolecithin)
	Steroid hormone biosynthesis	1	4-Methylpentanal
M2_Control	Arginine and proline metabolism	1	1-Pyrroline-5-carboxylic acid, 1-Pyrroline-2-carboxylic acid
	Alanine, aspartate and glutamate metabolism	1	1-Pyrroline-5-carboxylic acid
	Valine, leucine and isoleucine degradation	1	FA 5:1;O (3-methyl-2-oxo-butanoic acid)
	Isoprenoid/cholesterol biosynthetic pathway	1	Farnesol
	Steroid biosynthesis	1	ST 27:3;O
	Ether lipid metabolism	1	LPC O-18:0
	Glycerophospholipid metabolism	1	PC 35:4, PE 38:4
	Linoleic acid metabolism	1	PC 35:4
	alpha-Linolenic acid metabolism	1	PC 35:4
	Arachidonic acid metabolism	1	PC 35:4
Sphingolipid metabolism	1	SM 40:1;O2	

4 Discussion

Experimental evidence for possible effects of EBOV on the metabolomes of affected cells has been scarce so far. With an untargeted metabolomics approach, in the current study, we show that exposure to Ebola VLP leads to metabolic changes in ECs and M1/M2 macrophages. Multiple pathways were also observed either upregulated or downregulated in each cell type.

Ebola VLP-treated ECs were mainly characterized by an alteration of lipids, fatty acids (FA), glycerophospholipids (GPL), sterol lipids (ST), and acylcarnitine (CAR) as can be seen in **Figure 3A**. Previous analysis of plasma lipidome changes in Ebola-infected patients has revealed the essential role of lipid for the disease outcome and state, due to their function as membrane structural components, signaling molecules, and energy sources [41]. In agreement, we found an upregulation of FAs, especially involved in several FA metabolism pathways, namely FA 9:1;O, FA 10:0, FA 10:1;O, FA 12:1;O, FA 16:1;O, FA 18:2 (linoleic acid), FA 18:2;O, FA 18:2;O3, FA 18:3;O, FA 20:0;O (thromboxane), FA 20:4 (arachidonic acid), FA 22:0 (docosanoic acid), and FAL 16:0. There is substantial evidence that FAs have a critical role in mediating vascular ECs dysfunction via contributing to, for example, nitric oxide production, oxidative stress, inflammation, apoptosis, etc. [42, 43]. It has also been demonstrated that FA (e.g., linoleic, arachidonic, eicosapentaenoic, docosahexaenoic acids) can function as endogenous defense against a variety of invading microorganisms but at the same time can act as immunomodulating agents to cause inflammation [44, 45]. Among GPL, our results show that the expression of phosphatidic acids (PA; PA 40:4 and PA 44:4), phosphatidylcholines (PC; PC 39:0, PC 40:1, and PC O-42:4), phosphatidylethanolamines (PE; PE 29:1 and PE 42:0), and phosphatidylserines (PS; PS 37:2) is induced in Ebola VLP-treated ECs. PA is involved in the regulation of membrane dynamics (fusion and fission events) [46], EBOV requires fusion of viral and cellular membranes mediated by Ebola GPs, which is solely responsible for virus-host membrane fusion machine required for virus entry into cells [47, 48]. In addition, PC is an important composite of cellular membranes [49]; a plasma

lipidome study revealed PC level is significantly enhanced in Ebola infection survivors compared to fatalities [41]. Similarly, increase in PE plasma levels was reported as signature of EBOV infection [50]. In addition to FA and GPL, impaired steroid secretion is reported in EBOV infection [51]; however, the results here show an upregulation of ST in ECs after treatment. This may indicate the potential host defense function to counteract EBOV due to their ability of reducing inflammation and suppressing the increase in vascular permeability [52, 53]. Our data also shows that treated ECs have higher levels of CAR, which are essential intermediates for fatty acid β -oxidation and organic acid metabolism [54]. This tendency was also found in Dengue fever patients compared to healthy control in a previous serum metabolome study [55]. The elevated levels of CAR may indicate a disturbed energy metabolism in ECs upon Ebola VLP treatment.

A relative reduction of amino acids, purine nucleotides, and carbohydrate metabolites involved in multiple metabolic pathways was identified in Ebola VLP-treated ECs compared to non-treated. The amino acids found here have strong association with the metabolism of gluconic amino acids (GAAs), including alanine, aspartate, and glutamate metabolism; arginine and proline metabolism; arginine biosynthesis; histidine metabolism; glutamine and glutamate metabolism; and glutathione metabolism. This may suggest that Ebola VLP-treated ECs display a drastic decrease in GAAs, which may reflect an upregulation of gluconeogenesis. Similarly, a decrease in the levels of most identified purine nucleotides and carbohydrates involved in purine metabolism, which are considered as a source of energy, was observed in treated ECs. The data may indicate a higher energy cost status in Ebola VLP-treated ECs, consistent with the results in a previous Ebola VLP-treated macrophages study [9].

Our results show that ST and FA are the two pre-eminent metabolite classes in both Ebola VLP-treated M1 and M2 groups. The change in ST metabolites is probably due to the involvement of steroid degradation and biosynthesis pathways in M1 and M2, respectively, according to our pathway analysis results. This is corroborated by a gene expression study

that reported upregulation of the steroid hormone metabolism pathway in Ebola infected primary human macrophages [9]. Multiple studies have demonstrated that steroids have miscellaneous effects on the survival and phagocytic activity of macrophages, especially the polarization of pro-inflammatory M1 phenotype macrophages to anti-inflammatory M2 [56-59]. As for FA, they can be released and utilized for the formation of pro-inflammatory molecules that enhance the phagocytic action of M1 macrophages in the initial stages of microorganisms invading [44]. Most of the FA found in treated M2 are involved in arachidonic acid metabolism, which was also previously reported to be upregulated in the induction of M2 polarization [60]. Arachidonic acid is a key inflammatory intermediate and known to have a critical role in immune response; for example, it modulates the polarization and function of macrophages for anti-microbial subtype, inactivates enveloped viruses, inhibits fatty acid synthesis that is critical for microbes to survive, and aids in the resolution of inflammation [44, 61]. A recent clinical study also showed the elevated trend of arachidonic acid in the serum of primary Dengue-infected patients [55]. The upregulation of the arachidonic acid metabolism pathway detected in M2, may be responsible for elevating the inflammatory response, which is beneficial for host defense against EBOV. According to previous findings that M1 polarization of macrophages is able to inhibit EBOV infection while M2 polarization can enhance infection [5, 8], the ST and FA metabolites found here may contribute to retaining their polarization and function to counteract EBOV. This hypothesis is also supported by the evidence that these two classes of lipids were detected in lower levels in the M1 and M2 control group. Moreover, reduced levels of triacylglycerols (TG) were observed in treated M2 groups. TG is a class of lipid that plays an important antibacterial role and the inhibition of its synthesis negatively affects the production of proinflammatory cytokines and macrophage phagocytic capacity [62, 63]. This is consistent with the promoting feature of M2 for Ebola and the results found here. Additionally, dityrosine was detected in the treated M2 group, which is a biomarker for elevated levels of oxidative stress. In which, oxidative stress has an association with a decreased macrophage response capacity to pathogens [64, 65], this may further support

the involvement of M2 in Ebola. While in Ebola VLP-treated M1 several lipids were detected, certain lipids, including LPC 18:0, 5,6-epoxy,18R-HEPE and N-arachidonoylglycine are reported as bioactive lipids. These bioactive lipids can be further metabolized to mediators that participate in the pro-inflammatory signaling and as a result contribute to a pro-inflammatory phenotype of circulating monocytes [66-69]. Such evidence may indicate that M1 macrophages tightly coordinate their metabolic programs to support immunological functions to counteract EBOV. In addition, platelet-activating factor (PAF) was observed in treated M1, which is a potent and versatile mediator of inflammation response to allergens and infectious processes, as well as the further recruitment of leukocytes and increase of vascular permeability [70]. This release of PAF from M1 was previously reported in macrophages obtained from Dengue-infected patients [71]. It was also proposed as a potential diagnostic and prognostic biomarker candidate for Lassa fever patients [72, 73].

It's worth noting that this work serves as the initial step towards understanding the potential metabolic alterations done to host cells upon Ebola exposure; however, the study has certain limitations that will be addressed in the future. Ebola GP is a key mediator of Ebola pathogenesis and determinant of disease severity [74, 75]. It has been suggested to have a key role in activating endothelial cells directly and decreasing endothelial barrier function [76]. Studies also show that GP is critical for initiating a sufficient signal for the activation of macrophages [9, 77]. It is of interest to gain further insight how GP alone contributes to cellular metabolic changes. The Ebola VLPs used in this work are composed of GPs, matrix proteins, and nucleoprotein, which are morphologically similar to the live virus and highly immunogenic, enabling us to have a comprehensive understanding of host cell response. Future complementary experiments (e.g., VLPs without GP, GP or matrix protein VP40 only) will contribute to better mechanistic understanding of the observed metabolic changes. While DI-MS has multiple advantages, mainly, high sample throughput capability, enhanced reproducibility, reduced time of analysis, and wide metabolic coverage making it best suited for untargeted metabolomics [78], its limitations also need to be taken into account. One limitation is the inability to distinguish between

the structural isomers of certain metabolites. In addition, it is more susceptible to ion suppression due to the lack of a separation technique and it lacks sufficient evidence to confirm possible structural elucidation, especially in the case of lipids. Thus, further large-scale studies involving targeted and quantitative analytical platforms are required to confirm the metabolomic alterations as well as potential biomarkers detected using untargeted metabolomics studies. In addition, other omics approaches (i.e., transcriptomics and proteomics) can be applied to reach a more complete disclosure of the mechanisms by which EBOV can affect the host response that contributes to disease pathology. In addition, the Ebola VLP used here is composed of nucleoprotein, glycoprotein, and matrix proteins. Although it does not contain the viral genes necessary for replication, it is morphologically and antigenically similar to wild-type EBOV and has been proven to be useful tools to study early events of EBOV pathogenesis [77, 79]. It allows us to disentangle the contribution of viral proteins to host cells from the contributions of host immunity and the process of infection.

In summary, an untargeted metabolomics analysis was undertaken and found metabolite and metabolic pathway alterations that are involved in the Ebola VLP-induced cellular metabolic reprogramming to ECs, M1, and M2. These results may pave the way towards identifying potential biomarkers that can predict Ebola disease progression, severity, and outcome, which may be helpful for diagnostics efforts. In addition, upon further confirmation and more targeted analysis, the abovementioned metabolic pathways may represent potential candidate targets for future development of prophylactic or therapeutic countermeasures. Ultimately, these findings may expand our knowledge of EBOV-induced metabolic alterations at the cellular level and aid in further investigation on systemic alterations.

Author Contribution

AM conceived and supervised the study. HT and YA conducted the experiments, analyzed the data, and wrote the manuscript. YS provided access to the mass spectrometer. THMO provided biological resources and macrophage preparations. All authors revised the manuscript and approved the final version.

Funding

H. T. is financially supported by the CSC Scholarship offered by the China Scholarship Council. A. M. and Y. A. acknowledge the support by the Leiden University Fund (W19340-5-EML).

Data Availability

Important data generated or analyzed during this study is included in this published article. Further information is available from the corresponding author on reasonable request.

Ethics approval and consent to participate

This study was approved by Sanquin' ethical advisory board and in accordance with the Declaration of Helsinki and according to Dutch legislation.

Competing Interests

The authors declare no competing interests.

References

1. Malvy D, McElroy AK, de Clerck H, Günther S, van Griensven J: **Ebola virus disease.** *The Lancet* 2019, **393**(10174):936-948.
2. Jacob ST, Crozier I, Fischer WA, Hewlett A, Kraft CS, Vega M-AdL, Soka MJ, Wahl V, Griffiths A, Bollinger L *et al*: **Ebola virus disease.** *Nature Reviews Disease Primers* 2020, **6**(1):13.
3. Weyer J, Grobbelaar A, Blumberg L: **Ebola Virus Disease: History, Epidemiology and Outbreaks.** *Current Infectious Disease Reports* 2015, **17**(5):21.
4. Mayhew SH, Kyamusugulwa PM, Kihangi Bindu K, Richards P, Kiyungu C, Balabanova D: **Responding to the 2018-2020 Ebola Virus Outbreak in the Democratic Republic of the Congo: Rethinking Humanitarian Approaches.** *Risk management and healthcare policy* 2021, **14**:1731-1747.
5. Rogers KJ, Maury W: **The role of mononuclear phagocytes in Ebola virus infection.** *Journal of Leukocyte Biology* 2018, **104**(4):717-727.
6. Falasca L, Agrati C, Petrosillo N, Di Caro A, Capobianchi MR, Ippolito G, Piacentini M: **Molecular mechanisms of Ebola virus pathogenesis: focus on cell death.** *Cell Death & Differentiation* 2015, **22**(8):1250-1259.
7. Bradley JH, Harrison A, Corey A, Gentry N, Gregg RK: **Ebola virus secreted glycoprotein decreases the anti-viral immunity of macrophages in early inflammatory responses.** *Cellular Immunology* 2018, **324**:24-32.
8. Rogers KJ, Brunton B, Mallinger L, Bohan D, Sevcik KM, Chen J, Ruggio N, Maury W: **IL-4/IL-13 polarization of macrophages enhances Ebola virus glycoprotein-dependent infection.** *PLOS Neglected Tropical Diseases* 2019, **13**(12):e0007819.
9. Wahl-Jensen V, Kurz S, Feldmann F, Buehler LK, Kindrachuk J, DeFilippis V, da Silva Correia J, Früh K, Kuhn JH, Burton DR *et al*: **Ebola Virion Attachment and Entry into Human Macrophages Profoundly Effects Early Cellular Gene Expression.** *PLOS Neglected Tropical Diseases* 2011, **5**(10):e1359.

10. Verreck FAW, de Boer T, Langenberg DML, Hoeve MA, Kramer M, Vaisberg E, Kastelein R, Kolk A, de Waal-Malefyt R, Ottenhoff THM: **Human IL-23-producing type 1 macrophages promote but IL-10-producing type 2 macrophages subvert immunity to (myco)bacteria.** *Proceedings of the National Academy of Sciences of the United States of America* 2004, **101**(13):4560.
11. Han JC, Li QX, Fang JB, Zhang JY, Li YQ, Li SZ, Cheng C, Xie CZ, Nan FL, Zhang H *et al*: **GII.P16-GII.2 Recombinant Norovirus VLPs Polarize Macrophages Into the M1 Phenotype for Th1 Immune Responses.** *Frontiers in Immunology* 2021, **12**.
12. Savage ND, de Boer T, Walburg KV, Joosten SA, van Meijgaarden K, Geluk A, Ottenhoff THM: **Human Anti-Inflammatory Macrophages Induce Foxp3⁺GITR⁺CD25⁺ Regulatory T Cells, Which Suppress via Membrane-Bound TGFβ-1.** *The Journal of Immunology* 2008, **181**(3):2220.
13. Shapouri-Moghaddam A, Mohammadian S, Vazini H, Taghadosi M, Esmaili S-A, Mardani F, Seifi B, Mohammadi A, Afshari JT, Sahebkar A: **Macrophage plasticity, polarization, and function in health and disease.** *Journal of Cellular Physiology* 2018, **233**(9):6425-6440.
14. Verreck FAW, de Boer T, Langenberg DML, van der Zanden L, Ottenhoff THM: **Phenotypic and functional profiling of human proinflammatory type-1 and anti-inflammatory type-2 macrophages in response to microbial antigens and IFN-γ and CD40L-mediated costimulation.** *Journal of Leukocyte Biology* 2006, **79**(2):285-293.
15. Escudero-Pérez B, Volchkova VA, Dolnik O, Lawrence P, Volchkov VE: **Shed GP of Ebola Virus Triggers Immune Activation and Increased Vascular Permeability.** *PLOS Pathogens* 2014, **10**(11):e1004509.
16. Yang Z-y, Duckers HJ, Sullivan NJ, Sanchez A, Nabel EG, Nabel GJ: **Identification of the Ebola virus glycoprotein as the main viral determinant of vascular cell cytotoxicity and injury.** *Nature Medicine* 2000, **6**(8):886-889.

17. Wahl-Jensen VM, Afanasieva TA, Seebach J, Ströher U, Feldmann H, Schnittler H-J: **Effects of Ebola Virus Glycoproteins on Endothelial Cell Activation and Barrier Function.** *Journal of Virology* 2005, **79**(16):10442-10450.
18. Junaid A, Tang H, van Reeuwijk A, Abouleila Y, Wuelfroth P, van Duinen V, Stam W, van Zonneveld AJ, Hankemeier T, Mashaghi A: **Ebola Hemorrhagic Shock Syndrome-on-a-Chip.** *iScience* 2020, **23**(1):100765.
19. Hacke M, Björkholm P, Hellwig A, Himmels P, de Almodóvar CR, Brügger B, Wieland F, Ernst AM: **Inhibition of Ebola virus glycoprotein-mediated cytotoxicity by targeting its transmembrane domain and cholesterol.** *Nature Communications* 2015, **6**(1):7688.
20. Wolf T, Kann G, Becker S, Stephan C, Brodt H-R, de Leuw P, Grünewald T, Vogl T, Kempf VAJ, Keppler OT *et al*: **Severe Ebola virus disease with vascular leakage and multiorgan failure: treatment of a patient in intensive care.** *The Lancet* 2015, **385**(9976):1428-1435.
21. Moni BM, Sakurai Y, Yasuda J: **Ebola Virus GP Activates Endothelial Cells via Host Cytoskeletal Signaling Factors.** *Viruses* 2022, **14**(1).
22. Evers TMJ, Holt LJ, Alberti S, Mashaghi A: **Reciprocal regulation of cellular mechanics and metabolism.** *Nature Metabolism* 2021, **3**(4):456-468.
23. Lévy P, Bartosch B: **Metabolic reprogramming: a hallmark of viral oncogenesis.** *Oncogene* 2016, **35**(32):4155-4164.
24. Thyrsted J, Holm CK: **Virus-induced metabolic reprogramming and innate sensing hereof by the infected host.** *Current Opinion in Biotechnology* 2021, **68**:44-50.
25. Martín-Vicente M, González-Riaño C, Barbas C, Jiménez-Sousa MÁ, Brochado-Kith O, Resino S, Martínez I: **Metabolic changes during respiratory syncytial virus infection of epithelial cells.** *PLOS ONE* 2020, **15**(3):e0230844.
26. De Smet J, Zimmermann M, Kogadeeva M, Ceyssens P-J, Vermaelen W, Blasdel B, Bin Jang H, Sauer U, Lavigne R: **High coverage metabolomics analysis reveals**

- phage-specific alterations to *Pseudomonas aeruginosa* physiology during infection.** *The ISME Journal* 2016, **10**(8):1823-1835.
27. Tiwari S, Dhole TN: **Metabolomics of Rhabdomyosarcoma Cell During Echovirus 30 Infection.** *Virology Journal* 2017, **14**(1):144.
28. Cheng M-L, Chien K-Y, Lai C-H, Li G-J, Lin J-F, Ho H-Y: **Metabolic Reprogramming of Host Cells in Response to Enteroviral Infection.** *Cells* 2020, **9**(2).
29. Smallwood HS, Duan S, Morfouace M, Rezinciuc S, Shulkin BL, Shelat A, Zink EE, Milasta S, Bajracharya R, Oluwaseun AJ *et al*: **Targeting Metabolic Reprogramming by Influenza Infection for Therapeutic Intervention.** *Cell Reports* 2017, **19**(8):1640-1653.
30. Thai M, Graham Nicholas A, Braas D, Nehil M, Komisopoulou E, Kurdistani Siavash K, McCormick F, Graeber Thomas G, Christofk Heather R: **Adenovirus E4ORF1-Induced MYC Activation Promotes Host Cell Anabolic Glucose Metabolism and Virus Replication.** *Cell Metabolism* 2014, **19**(4):694-701.
31. Jordan TX, Randall G: **Flavivirus modulation of cellular metabolism.** *Current Opinion in Virology* 2016, **19**:7-10.
32. Thaker SK, Chapa T, Garcia G, Gong D, Schmid EW, Arumugaswami V, Sun R, Christofk HR: **Differential Metabolic Reprogramming by Zika Virus Promotes Cell Death in Human versus Mosquito Cells.** *Cell Metabolism* 2019, **29**(5):1206-1216.e1204.
33. Moolamalla STR, Balasubramanian R, Chauhan R, Priyakumar UD, Vinod PK: **Host metabolic reprogramming in response to SARS-CoV-2 infection: A systems biology approach.** *Microbial Pathogenesis* 2021, **158**:105114.
34. Kirwan JA, Weber RJM, Broadhurst DI, Viant MR: **Direct infusion mass spectrometry metabolomics dataset: a benchmark for data processing and quality control.** *Scientific Data* 2014, **1**(1):140012.

35. McMillan A, Renaud JB, Gloor GB, Reid G, Sumarah MW: **Post-acquisition filtering of salt cluster artefacts for LC-MS based human metabolomic studies.** *Journal of Cheminformatics* 2016, **8**(1):44.
36. Jolliffe IT, Cadima J: **Principal component analysis: a review and recent developments.** *Philosophical Transactions of the Royal Society A: Mathematical, Physical and Engineering Sciences* 2016, **374**(2065):20150202.
37. Bradley W, Robert P: **Multivariate Analysis in Metabolomics.** *Current Metabolomics* 2013, **1**(1):92-107.
38. Schymanski EL, Jeon J, Gulde R, Fenner K, Ruff M, Singer HP, Hollender J: **Identifying Small Molecules via High Resolution Mass Spectrometry: Communicating Confidence.** *Environmental Science & Technology* 2014, **48**(4):2097-2098.
39. Watson DG: **A ROUGH GUIDE TO METABOLITE IDENTIFICATION USING HIGH RESOLUTION LIQUID CHROMATOGRAPHY MASS SPECTROMETRY IN METABOLOMIC PROFILING IN METAZOANS.** *Computational and Structural Biotechnology Journal* 2013, **4**(5):e201301005.
40. Ivanisevic J, Want EJ: **From Samples to Insights into Metabolism: Uncovering Biologically Relevant Information in LC-HRMS Metabolomics Data.** *Metabolites* 2019, **9**(12).
41. Kyle JE, Burnum-Johnson KE, Wendler JP, Eisfeld AJ, Halfmann PJ, Watanabe T, Sahr F, Smith RD, Kawaoka Y, Waters KM *et al*: **Plasma lipidome reveals critical illness and recovery from human Ebola virus disease.** *Proceedings of the National Academy of Sciences* 2019, **116**(9):3919.
42. Ghosh A, Gao L, Thakur A, Siu PM, Lai CWK: **Role of free fatty acids in endothelial dysfunction.** *Journal of Biomedical Science* 2017, **24**(1):50.
43. Hennig B, Lei W, Arzuaga X, Ghosh DD, Saraswathi V, Toborek M: **Linoleic acid induces proinflammatory events in vascular endothelial cells via activation of**

- PI3K/Akt and ERK1/2 signaling.** *The Journal of Nutritional Biochemistry* 2006, **17**(11):766-772.
44. Das UN: **Arachidonic acid and other unsaturated fatty acids and some of their metabolites function as endogenous antimicrobial molecules: A review.** *Journal of Advanced Research* 2018, **11**:57-66.
45. Barberis E, Timo S, Amede E, Vanella VV, Puricelli C, Cappellano G, Raineri D, Cittone MG, Rizzi E, Pedrinelli AR *et al*: **Large-Scale Plasma Analysis Revealed New Mechanisms and Molecules Associated with the Host Response to SARS-CoV-2.** *International Journal of Molecular Sciences* 2020, **21**(22).
46. Kooijman EE, Carter KM, van Laar EG, Chupin V, Burger KNJ, de Kruijff B: **What Makes the Bioactive Lipids Phosphatidic Acid and Lysophosphatidic Acid So Special?** *Biochemistry* 2005, **44**(51):17007-17015.
47. Das DK, Bulow U, Diehl WE, Durham ND, Senjobe F, Chandran K, Luban J, Munro JB: **Conformational changes in the Ebola virus membrane fusion machine induced by pH, Ca²⁺, and receptor binding.** *PLOS Biology* 2020, **18**(2):e3000626.
48. Freitas MS, Gaspar LP, Lorenzoni M, Almeida FCL, Tinoco LW, Almeida MS, Maia LF, Degreève L, Valente AP, Silva JL: **Structure of the Ebola Fusion Peptide in a Membrane-mimetic Environment and the Interaction with Lipid Rafts** ^{*}. *Journal of Biological Chemistry* 2007, **282**(37):27306-27314.
49. Zhang J, Zhang Z, Chukkapalli V, Nchoutmboube JA, Li J, Randall G, Belov GA, Wang X: **Positive-strand RNA viruses stimulate host phosphatidylcholine synthesis at viral replication sites.** *Proceedings of the National Academy of Sciences* 2016, **113**(8):E1064.
50. Einfeld AJ, Halfmann PJ, Wendler JP, Kyle JE, Burnum-Johnson KE, Peralta Z, Maemura T, Walters KB, Watanabe T, Fukuyama S *et al*: **Multi-platform Omics Analysis of Human Ebola Virus Disease Pathogenesis.** *Cell Host & Microbe* 2017, **22**(6):817-829.e818.

51. Zhao J-M, Dong S-J, Li J, Ji J-S: **The Ebola epidemic is ongoing in West Africa and responses from China are positive.** *Military Medical Research* 2015, **2**(1):9.
52. Barnes PJ: **How corticosteroids control inflammation: Quintiles Prize Lecture 2005.** *British Journal of Pharmacology* 2006, **148**(3):245-254.
53. Bandara SMR, Herath HMMTB: **Corticosteroid actions on dengue immune pathology; A review article.** *Clinical Epidemiology and Global Health* 2020, **8**(2):486-494.
54. Rinaldo P, Cowan TM, Matern D: **Acylcarnitine profile analysis.** *Genetics in Medicine* 2008, **10**(2):151-156.
55. Cui L, Lee YH, Kumar Y, Xu F, Lu K, Ooi EE, Tannenbaum SR, Ong CN: **Serum Metabolome and Lipidome Changes in Adult Patients with Primary Dengue Infection.** *PLOS Neglected Tropical Diseases* 2013, **7**(8):e2373.
56. Chakraborty S, Pramanik J, Mahata B: **Revisiting steroidogenesis and its role in immune regulation with the advanced tools and technologies.** *Genes & Immunity* 2021, **22**(3):125-140.
57. Desgeorges T, Caratti G, Mounier R, Tuckermann J, Chazaud B: **Glucocorticoids Shape Macrophage Phenotype for Tissue Repair.** *Frontiers in Immunology* 2019, **10**:1591.
58. Ehrchen JM, Roth J, Barczyk-Kahlert K: **More Than Suppression: Glucocorticoid Action on Monocytes and Macrophages.** *Frontiers in Immunology* 2019, **10**:2028.
59. Ikezumi Y, Kondoh T, Matsumoto Y, Kumagai N, Kaneko M, Hasegawa H, Yamada T, Kaneko U, Nikolic-Paterson DJ: **Steroid treatment promotes an M2 anti-inflammatory macrophage phenotype in childhood lupus nephritis.** *Pediatric Nephrology* 2021, **36**(2):349-359.
60. Xu M, Wang X, Li Y, Geng X, Jia X, Zhang L, Yang H: **Arachidonic Acid Metabolism Controls Macrophage Alternative Activation Through Regulating Oxidative Phosphorylation in PPAR γ Dependent Manner.** *Frontiers in Immunology* 2021, **12**:2040.

61. He L, Zhu D, Liang X, Li Y, Liao L, Yang C, Huang R, Zhu Z, Wang Y: **Multi-Omics Sequencing Provides Insights Into Age-Dependent Susceptibility of Grass Carp (*Ctenopharyngodon idellus*) to Reovirus.** *Frontiers in Immunology* 2021, **12**:2396.
62. Morgan PK, Huynh K, Pernes G, Miotto PM, Mellett NA, Giles C, Meikle PJ, Murphy AJ, Lancaster GI: **Macrophage polarization state affects lipid composition and the channeling of exogenous fatty acids into endogenous lipid pools.** *Journal of Biological Chemistry* 2021, **297**(6):101341.
63. Castoldi A, Monteiro LB, van Teijlingen Bakker N, Sanin DE, Rana N, Corrado M, Cameron AM, Hässler F, Matsushita M, Caputa G *et al*: **Triacylglycerol synthesis enhances macrophage inflammatory function.** *Nature Communications* 2020, **11**(1):4107.
64. DiMarco T, Giulivi C: **Current analytical methods for the detection of dityrosine, a biomarker of oxidative stress, in biological samples.** *Mass Spectrometry Reviews* 2007, **26**(1):108-120.
65. de Groot LES, van der Veen TA, Martinez FO, Hamann J, Lutter R, Melgert BN: **Oxidative stress and macrophages: driving forces behind exacerbations of asthma and chronic obstructive pulmonary disease?** *American Journal of Physiology-Lung Cellular and Molecular Physiology* 2018, **316**(2):L369-L384.
66. Chiurchiù V, Leuti A, Maccarrone M: **Bioactive Lipids and Chronic Inflammation: Managing the Fire Within.** *Frontiers in Immunology* 2018, **9**.
67. Yoder M, Zhuge Y, Yuan Y, Holian O, Kuo S, van Breemen R, Thomas LL, Lum H: **Bioactive Lysophosphatidylcholine 16:0 and 18:0 Are Elevated in Lungs of Asthmatic Subjects.** *Allergy Asthma Immunol Res* 2014, **6**(1):61-65.
68. Bradshaw HB, Rimmerman N, Hu SS-J, Benton VM, Stuart JM, Masuda K, Cravatt BF, O'Dell DK, Walker JM: **The endocannabinoid anandamide is a precursor for the signaling lipid N-arachidonoyl glycine by two distinct pathways.** *BMC Biochemistry* 2009, **10**(1):14.

69. Leishman E, Mackie K, Bradshaw HB: **Elevated Levels of Arachidonic Acid-Derived Lipids Including Prostaglandins and Endocannabinoids Are Present Throughout ABHD12 Knockout Brains: Novel Insights Into the Neurodegenerative Phenotype.** *Frontiers in Molecular Neuroscience* 2019, **12**.
70. Klein M, Dao V, Khan F: **A Review of Platelet-Activating Factor As a Potential Contributor to Morbidity and Mortality Associated with Severe COVID-19.** *Clinical and Applied Thrombosis/Hemostasis* 2021, **27**:10760296211051764.
71. Souza DG, Fagundes CT, Sousa LP, Amaral FA, Souza RS, Souza AL, Kroon EG, Sachs D, Cunha FQ, Bukin E *et al*: **Essential role of platelet-activating factor receptor in the pathogenesis of Dengue virus infection.** *Proceedings of the National Academy of Sciences* 2009, **106**(33):14138.
72. Gale TV, Horton TM, Grant DS, Garry RF: **Metabolomics analyses identify platelet activating factors and heme breakdown products as Lassa fever biomarkers.** *PLOS Neglected Tropical Diseases* 2017, **11**(9):e0005943.
73. Gale TV, Schieffelin JS, Branco LM, Garry RF, Grant DS: **Elevated I-threonine is a biomarker for Lassa fever and Ebola.** *Virology Journal* 2020, **17**(1):188.
74. Lee JE, Saphire EO: **Ebolavirus glycoprotein structure and mechanism of entry.** *Future Virology* 2009, **4**(6):621-635.
75. Mohan Gopi S, Ye L, Li W, Monteiro A, Lin X, Sapkota B, Pollack Brian P, Compans Richard W, Yang C: **Less Is More: Ebola Virus Surface Glycoprotein Expression Levels Regulate Virus Production and Infectivity.** *Journal of Virology* 2014, **89**(2):1205-1217.
76. Moni BM, Sakurai Y, Yasuda J: **Ebola Virus GP Activates Endothelial Cells via Host Cytoskeletal Signaling Factors.** In: *Viruses*. vol. 14; 2022.
77. Wahl-Jensen V, Kurz Sabine K, Hazelton Paul R, Schnittler H-J, Ströher U, Burton Dennis R, Feldmann H: **Role of Ebola Virus Secreted Glycoproteins and Virus-Like Particles in Activation of Human Macrophages.** *Journal of Virology* 2005, **79**(4):2413-2419.

78. González-Domínguez R, Sayago A, Fernández-Recamales Á: **Direct infusion mass spectrometry for metabolomic phenotyping of diseases.** *Bioanalysis* 2016, **9(1):131-148.**
79. Warfield Kelly L, Bosio Catharine M, Welcher Brent C, Deal Emily M, Mohamadzadeh M, Schmaljohn A, Aman MJ, Bavari S: **Ebola virus-like particles protect from lethal Ebola virus infection.** *Proceedings of the National Academy of Sciences* 2003, **100(26):15889-15894.**

Supplementary Information

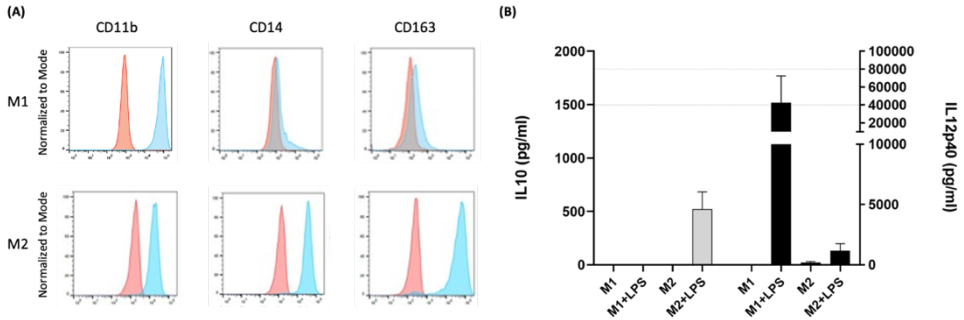


Figure S1. Characterization of human M1 and M2 macrophages. (A) CD11b is relatively high on M1, while CD14 and CD163 are expressed consistently higher on M2 (red: unstained sample; blue: stained sample). (B) After stimulation with LPS, the IL-10 production by M2 is significantly higher than by M1, while M1 secretes high levels of IL-12.

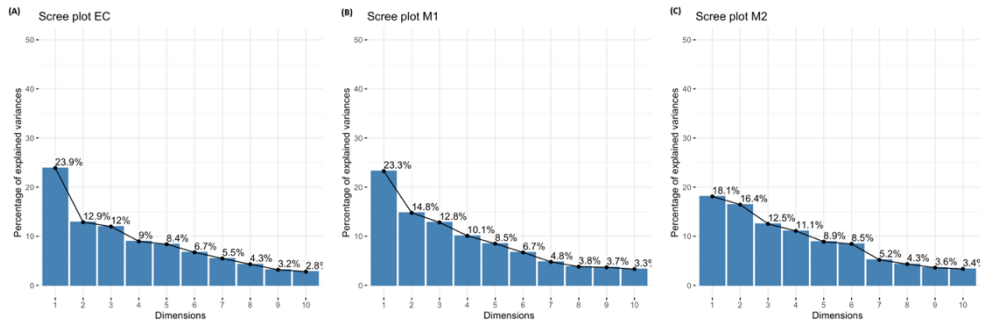


Figure S2. Scree plot shows the variance explained by the top 10 principal components in ECs, M1 and M2 after treatment with Ebola VLPs.

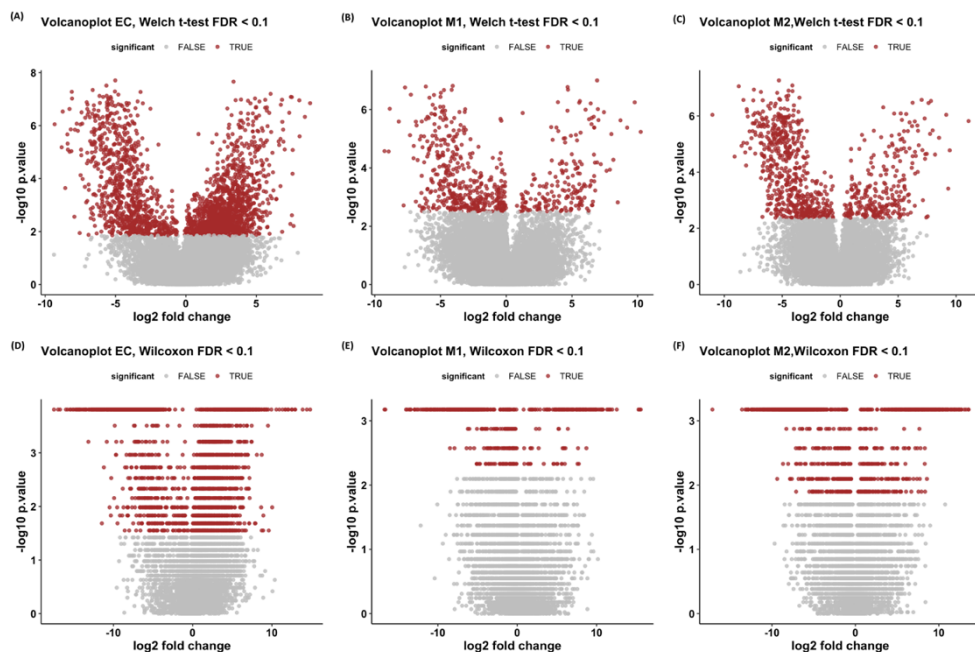


Figure S3. Volcano plot of the differentially abundant peaks in ECs, M1 and M2 after treatment with/without Ebola VLPs. The graphs plot the relative abundance of peaks against their statistical significance, respectively reported as \log_2 fold change values of the average of mean peak intensity against the respective $-\log_{10}$ adjusted p -values, in ECs (A & D), M1 (B & E), and M2 (C & F). Peaks with an adjusted p -value of less than 0.1 are shown as significant. Peaks with a \log_2 fold change less than -1 are attributed to control or treated and peaks with a \log_2 fold change of greater than 1 are attributed to control or treated.

Table S1. Putatively identified metabolites and lipids in control group of ECs (Welch's *t*-test)

Compound name	m/z	P-value	P.adjust	Formula	Adduct	Pathway/Class
FA 5:1	123.0418	0.00267356	0.034064161	C5H8O2	[M+Na] ¹⁺	Fatty acyl
Dihydrothymine	129.066	1.5094E-05	0.000731182	C5H8N2O2	[M+H] ¹⁺	Pyrimidine metabolism
FA 8:1	165.0884	0.00670805	0.062451625	C8H14O2	[M+Na] ¹⁺	Fatty acyl
FA 11:0;O	225.1459	0.00802811	0.069271501	C11H22O3	[M+Na] ¹⁺	Fatty acyl
FA 7:1	151.0728	0.00991551	0.079844633	C7H12O2	[M+Na] ¹⁺	Fatty acyl
FA 6:1;O	153.0519	0.0078403	0.068113797	C6H10O3	[M+Na] ¹⁺	Fatty acyl
FAL 9:2	161.0934	0.00548446	0.054530476	C9H14O1	[M+Na] ¹⁺	Fatty acyl (fatty aldehyde)

Table S2. Putatively identified metabolites and lipids in control group of ECs (Wilcoxon rank-sum test)

Compound name	m/z	P-value	P.adjust	Formula	Adduct	Pathway/Class
L-Aspartic acid	172.0006	0.00699301	0.03200558	C4H7N1O4	[M+K]1+	Alanine, aspartate and glutamate metabolism, Arginine biosynthesis, Histidine metabolism
L-Glutamic acid	186.0161*	0.004662	0.02254342	C5H9N1O4	[M+K]1+	Alanine, aspartate and glutamate metabolism, Arginine biosynthesis, Histidine metabolism, Glutamine and glutamate metabolism, Glutathione metabolism
L-4-Hydroxyglutamate semialdehyde						Arginine and proline metabolism
FA 5:2;O2	148.0603	0.02066822	0.07690692	C5H6O4	[M+NH4]1+	Fatty acyl (methyl branched FA)
FA 22:5;O2	385.2345	0.00062216	0.00381612	C22H34O4	[M+Na]1+	Fatty acyls
FOH 9:2	163.1091	0.02066822	0.07690692	C9H16O1	[M+Na]1+	Fatty acyls (fatty alcohols)
FOH 6:0;O4	167.0911	0.01041181	0.04417036	C6H14O5	[M+H]1+	Fatty acyls (fatty alcohols)
FAL 17:3	249.2212	0.02812743	0.09756647	C17H28O1	[M+H]1+	Fatty acyls (fatty aldehydes)
Stearamide	306.2762	0.0001554	0.00107675	C18H37N1O1	[M+Na]1+	Fatty acyls (fatty amides)
gamma-Glutamyvaline	269.1103	0.02812743	0.09756647	C10H18N2O5	[M+Na]1+	Glutathione metabolism
Glutamyllysine	298.1369	0.00062216	0.00381612	C11H21N3O5	[M+Na]1+	Glutathione metabolism
Glutathione†	308.0904	0.0010878	0.00630182	C10H17N3O6S1	[M+H]1+	Glutathione metabolism
	330.0719	0.00062216	0.00381612		[M+Na]1+	
DG 30:2	575.4086	0.0001554	0.00107675	C33H60O5	[M+K]1+	Glycerolipids (Diradylglycerols)
TG 44:0	768.7058	0.0001554	0.00107675	C47H90O6	[M+NH4]1+	Glycerolipids (Triadylglycerols)

TG 46:0	796.7357	0.0003108	0.00205198	C49H94O6	[M++NH4]1+	Glycerolipids (Triradylglycerols)
FA 5:0;O2	157.0469	0.01476301	0.05898888	C5H10O4	[M++Na]1+	Fatty acyls
Deoxyadenosine monophosphate (DAMP)	332.0765	0.0006216	0.00381612	C10H14N5O6P1	[M++H]1+	Purine metabolism
N-Acetylneuraminic acid	348.0698*	0.02066822	0.07690692	C11H19N1O9	[M++K]1+	Purine metabolism
2'-Deoxyguanosine monophosphate				C10H14N5O7P1	[M++H]1+	
Adenosine 2'-phosphate (AMP)						
2-hydroxy-dAMP						
Adenosine 3',5'-diphosphate	450.0175*	0.0029526	0.01517475	C10H15N5O10P2	[M++Na]1+	Purine metabolism
dGDP						
ADP						
UDP-GlcNAc	630.0703	0.02066822	0.07690692	C17H27N3O17P2	[M++Na]1+	Saccharolipids (Acylaminosugars)
N-Acetyserine	186.0161	0.004662	0.02254342	C5H9N1O4	[M++K]1+	Amino acid
Glycerylphosphorylethanolamine	238.0445	0.0001554	0.00107675	C5H14N1O6P1	[M++Na]1+	Glycerophospholipids
gamma-Glutamyllysine	298.1369	0.0006216	0.00381612	C11H21N3O5	[M++Na]1+	Amino acid
FA 22:5;O2 (19,20-DIHDPA)	385.2345	0.0006216	0.00381612	C22H34O4	[M++Na]1+	Fatty acyl
ST 24:2;O4	429.2398	0.0001554	0.00107675	C24H38O4	[M++K]1+	Sterol lipid (bile acid)

(*) is an m/z with more than one possible database match, (†) is a database hit detected as multiple adducts

Table S3. Putatively identified metabolites and lipids in Ebola VLP treatment group of ECs (Welch's *t*-test)

Compound name	m/z	P-value	P.adjust	Formula	Adduct	Pathway/Class
PS 37:2	802.5572	0.00022855	0.005978249	C43H80N1O10P1	[M+H] ¹⁺	Glycerophospholipid
PA 44:4	847.5615	1.06145E-05	0.000549323	C47H85O8P1	[M+K] ¹⁺	Glycerophospholipid
PC 39:0	870.6356*	1.29559E-05	0.00064166	C47H94N1O8P1	[M+K] ¹⁺	Glycerophospholipid
PE 42:0						
ST 19:0:O2	315.2308*	0.00173361	0.025326252	C19H32O2	[M+Na] ¹⁺	Sterol lipids
ST 21:3:O2 (progesterone)				C21H30O2	[M+H] ¹⁺	Steroid hormone biosynthesis/Sterol lipids

(*) is an m/z with more than one possible database match

Table S4. Putatively identified metabolites and lipids in Ebola VLP treatment group of ECs (Wilcoxon rank-sum test)

Compound name	m/z	P-value	P.adjust	Formula	Adduct	Pathway/Class
Arachidonic acid(FA 20:4)	305.2472	0.000155	0.001077	C20H32O2	[M+H] ¹⁺	Arachidonic acid metabolism, Linoleic acid metabolism, Biosynthesis of unsaturated fatty acids
N-Decanoylglycine	230.1747	0.000155	0.001077	C12H23NO3	[M+H] ¹⁺	Acylglycine
N-Undecanoylglycine	244.1904	0.000155	0.001077	C13H25NO3	[M+H] ¹⁺	Acylglycine
FA 9:1;O	173.1172	0.000155	0.001077	C9H16O3	[M+H] ¹⁺	alpha-Linolenic acid metabolism/Fatty acyl
FA 18:3;O†	312.2528	0.000155	0.001077	C18H30O3	[M+NH4] ¹⁺	alpha-Linolenic acid metabolism/Fatty acyl
	295.2257	0.010412	0.04417	C18H30O3	[M+H] ¹⁺	
FA 20:0;O	297.3139	0.000155	0.001077	C20H40O1	[M+H] ¹⁺	Arachidonic acid metabolism/eicosanoids
(Thromboxane)†	351.2863	0.000155	0.001077	C20H40O3	[M+Na] ¹⁺	
ST 27:1;O3	436.3771	0.000155	0.001077	C27H46O3	[M+NH4] ¹⁺	Bile acid biosynthesis/sterol lipids
FA 22:0 (Docosanoic acid)	358.3663	0.000155	0.001077	C22H44O2	[M+NH4] ¹⁺	Biosynthesis of unsaturated fatty acids/fatty acyl
FA 10:0	173.1535	0.000155	0.001077	C10H20O2	[M+H] ¹⁺	Fatty acid biosynthesis
FA 10:1;O	187.1326	0.000155	0.001077	C10H18O3	[M+H] ¹⁺	Fatty acid biosynthesis/Fatty acyl
trans-Dodec-2-enoic acid	216.1952	0.000155	0.001077	C12H22O2	[M+NH4] ¹⁺	Fatty acid biosynthesis/Fatty acyl
FA 12:1;O (3-oxo-dodecanoic acid)	232.1903	0.000155	0.001077	C12H22O3	[M+NH4] ¹⁺	Fatty acid biosynthesis/fatty acyl
FA 16:1;O	288.2529	0.000155	0.001077	C16H30O3	[M+NH4] ¹⁺	Fatty acid biosynthesis/fatty acyl
trans-2-Hexenoic acid	115.0756	0.000155	0.001077	C6H10O2	[M+H] ¹⁺	Fatty acyl
FA 8:0;O	161.1169	0.000155	0.001077	C8H16O3	[M+H] ¹⁺	Fatty acyl
FA 12:1	216.1952	0.000155	0.001077	C12H22O2	[M+NH4] ¹⁺	Fatty acyl
FA 18:1	283.2631	0.000155	0.001077	C18H34O2	[M+H] ¹⁺	Fatty acyl
FA 5:0	103.0755	0.000155	0.001077	C5H10O2	[M+H] ¹⁺	Fatty acyl

FA 6:2	113.06	0.000155	0.001077	C6H8O2	[M+H] ¹⁺	Fatty acyl
FA 6:1	115.0756	0.000155	0.001077	C6H10O2	[M+H] ¹⁺	Fatty acyl
FA 5:0	119.0704	0.000155	0.001077	C5H10O3	[M+H] ¹⁺	Fatty acyl
FA 6:0	133.0859	0.000155	0.001077	C6H12O3	[M+H] ¹⁺	Fatty acyl
FA 8:1	143.1066	0.000155	0.001077	C8H14O2	[M+H] ¹⁺	Fatty acyl
FA 8:0	161.1169	0.000155	0.001077	C8H16O3	[M+H] ¹⁺	Fatty acyl
FA 10:6	177.0543	0.000155	0.001077	C10H8O3	[M+H] ¹⁺	Fatty acyl
FA 14:2	242.2114	0.000155	0.001077	C14H24O2	[M+NH4] ¹⁺	Fatty acyl
FA 12:1:03	269.1355	0.000155	0.001077	C12H22O5	[M+Na] ¹⁺	Fatty acyl
FA 16:2	270.2422	0.000155	0.001077	C16H28O2	[M+NH4] ¹⁺	Fatty acyl
FA 16:1:02	287.2211	0.000155	0.001077	C16H30O4	[M+H] ¹⁺	Fatty acyl
FA 20:0	313.3092	0.000155	0.001077	C20H40O2	[M+H] ¹⁺	Fatty acyl
CAR 5:0	246.1697	0.000155	0.001077	C12H23N1O4	[M+H] ¹⁺	Fatty acyl (acyl carnitines)
CAR 7:0	274.2004	0.000155	0.001077	C14H27N1O4	[M+H] ¹⁺	Fatty acyl (acyl carnitines)
3-hydroxyundecanoyl carnitine	363.2865	0.000155	0.001077	C18H35N1O5	[M+NH4] ¹⁺	Fatty acyl (acyl carnitines)
CAR 20:0	456.403	0.000155	0.001077	C27H53N1O4	[M+H] ¹⁺	Fatty acyl (acyl carnitines)
CAR 4:1	230.1384	0.000155	0.001077	C11H19N1O4	[M+H] ¹⁺	Fatty acyl (acyl carnitines)
CAR 14:0	405.3339	0.000155	0.001077	C21H41N1O5	[M+NH4] ¹⁺	Fatty acyl (acyl carnitines)
CAR 18:0	445.4019	0.000155	0.001077	C25H49N1O4	[M+NH4] ¹⁺	Fatty acyl (acyl carnitines)
CAR 22:5	474.3564	0.000155	0.001077	C29H47N1O4	[M+H] ¹⁺	Fatty acyl (acyl carnitines)
FOH 8:5	121.0649	0.000155	0.001077	C8H8O1	[M+H] ¹⁺	Fatty acyl (fatty alcohols)
FOH 8:2	127.1119	0.000155	0.001077	C8H14O1	[M+H] ¹⁺	Fatty acyl (fatty alcohols)
FOH 8:5	138.0911	0.000155	0.001077	C8H8O1	[M+NH4] ¹⁺	Fatty acyl (fatty alcohols)
FAL 16:0 (Palmitaldehyde)	241.2524	0.000155	0.001077	C16H32O1	[M+H] ¹⁺	Fatty acyl (fatty aldehydes)/ Fatty acid degradation

FA 6:0	117.0911	0.000155	0.001077	C6H12O2	[M+H] ¹⁺	Fatty acyl (methyl branched)
DG(35:1)	626.572	0.000155	0.001077	C38H72O5	[M+NH4] ¹⁺	Glycerolipids (Diacylglycerol)
TG(52:3)	874.7831	0.000155	0.001077	C55H100O6	[M+NH4] ¹⁺	Glycerolipids (Triacylglycerol)
PE 29:1	670.4402	0.010412	0.04417	C34H66N1O8P1	[M+Na] ¹⁺	Glycerophospholipids
PA(40:4)	791.4963	0.000155	0.001077	C43H77O8P1	[M+K] ¹⁺	Glycerophospholipids
PC(40:1)	852.6828	0.010412	0.04417	C48H96N1O7P1	[M+Na] ¹⁺	Glycerophospholipids
FA 18:2,O	314.2682	0.000155	0.001077	C18H32O3	[M+NH4] ¹⁺	Lineolic acid metabolism/ fatty acyl
FA 18:2 (linoleic acid)	281.2477	0.000155	0.001077	C18H32O2	[M+H] ¹⁺	Lineolic acid metabolism/fatty acyl
PC(O-42:4) (lecithin)	852.6828	0.010412	0.04417	C50H94N1O7P1	[M+H] ¹⁺	Linoleic acid metabolism,Arachidonic acid metabolism, alpha-Linolenic acid metabolism, Glycerophospholipid metabolism
FA 18:2,O3 (9,12,13,TriHODE)	351.2139	0.000155	0.001077	C18H32O5	[M+Na] ¹⁺	Linoleic acid metabolism/fatty acyl
CDP-DG 25:0	856.4105	0.006993	0.032006	C37H67N3O15P2	[M+H] ¹⁺	Phospholipid metabolism/glycerophospholipid
ST 19:0,O	294.2781	0.000155	0.001077	C19H32O1	[M+NH4] ¹⁺	Sterol lipids
ST 20:4,O2	337.1553	0.000155	0.001077	C20H26O2	[M+K] ¹⁺	Sterol lipids
FA 5:1,O	117.0548	0.000155	0.001077	C5H8O3	[M+H] ¹⁺	Valine, leucine and isoleucine degradation, Valine, leucine and isoleucine biosynthesis, Pantothenate and CoA biosynthesis, lysine degradation

(†) is a database hit detected as multiple adducts

Table S5. Putatively identified metabolites and lipids in control group of M1 (Welch's *t*-test)

Compound name	m/z	P-value	P.adjust	Formula	Adduct	Pathway/Class
PC 30:1	704.5221*	0.00156	0.067956	C38H74N1O8P1	[M+H] ¹⁺	Glycerophospholipids
PE 33:1						
PC 32:2	730.5363*	0.00162	0.068856	C40H76N1O8P1	[M+H] ¹⁺	Glycerophospholipids
PE 35:2						
PE 34:2	716.5192*	0.000729	0.042668	C39H74N1O8P1	[M+H] ¹⁺	Glycerophospholipids
PA 36:3				C39H71O8P1	[M+NH4] ¹⁺	

(*) is an m/z with more than one possible database match

Table S6. Putatively identified metabolites and lipids in control group of M1 (Wilcoxon rank-sum test)

Compound name	m/z	P-value	P.adjust	Formula	Adduct	Pathway/Class
Oxoglutaric acid	164.0556	0.000666	0.0143396	C5H6O5	[M+NH4]1+	Citrate acid cycle
FA 22:3	335.2934	0.002664	0.0467845	C22H38O2	[M+H]1+	Fatty acyl
CAR 16:0 (L-palmitoylcarnitine)	417.3678	0.000666	0.0143396	C23H45N1O4	[M+NH4]1+	Fatty acid degradation pathway/acyl carnitine
SM 40:0;O2	811.6652	0.000666	0.0143396	C45H93N2O6P1	[M+Na]1+	Sphingolipids
FA 5:1	101.0599	0.000666	0.0143396	C5H8O2	[M+H]1+	Fatty acyl

Table S7. Putatively identified metabolites and lipids in Ebola VLP treatment group of M1 (Welch's *t*-test)

Compound name	m/z	P-value	P.adjust	Formula	Adduct	Pathway/Class
5-Androstene-3alpha-16b,17b-triol	329.2084	0.00131231	0.06151793	C19H30O3	[M+Na] ¹⁺	Steroids
Ubiquinol	343.1881	0.00057706	0.03630289	C19H28O4	[M+Na] ¹⁺	Ubiquinone and other terpenoid-quinone biosynthesis
CAR 18:2	424.342	0.0002082	0.01816914	C25H45N1O4	[M+H] ¹⁺	Acyl carnitine

Table S8. Putatively identified metabolites and lipids in Ebola VLP treatment group of M1 (Wilcoxon rank-sum test)

Compound name	m/z	P-value	P.adjust	Formula	Adduct	Pathway/Class
CAR 22:5	474.3564	0.000666	0.014339605	C29H47N1O4	[M+H] ¹⁺	Acyl carnitine
3-methyl-thiopropionic acid	121.0319	0.000666	0.014339605	C4H8O2S1	[M+H] ¹⁺	Cysteine and methionine metabolism/fatty acyl
Heptylmalonic acid	203.1275*	0.000666	0.014339605	C10H19O4	[M+H] ¹⁺	Fatty acyl
FA 10:1:O2						
3-Methylazelaic acid						
FA 12:0:O	217.1791	0.000666	0.014339605	C12H24O3	[M+H] ¹⁺	Fatty acyl
5,6-epoxy,18R-HEPE	355.1871*	0.001332	0.026117572	C20H28O4	[M+Na] ¹⁺	Fatty acyl (eicosanoid)
7'-Carboxy-gamma-tocotrienol						Benzopyrans (medium chain fatty acid)
FA 5:1:O2	150.0759	0.000666	0.014339605	C5H8O4	[M+NH4] ¹⁺	Fatty acyl /butanoate metabolism and pantothenate and CoA biosynthesis pathways
N-Arachidonoylglycine	362.2693	0.000666	0.014339605	C22H35N1O3	[M+H] ¹⁺	Fatty amides
LPC 18:0	524.3713	0.000666	0.014339605	C26H55N1O7P1	[M+H] ¹⁺	Glycerophospholipid metabolism/Glycerophospholipids
PG 42:10	865.499	0.000666	0.014339605	C48H75O10P1	[M+Na] ¹⁺	Glycerophospholipids
PC O-18:0 (Platelet-activating factor)	524.3713	0.000666	0.014339605	C26H54N1O7P1	[M+H] ¹⁺	Glycerophospholipids
ST 19:2:O2	289.2159	0.000666	0.014339605	C19H28O2	[M+H] ¹⁺	Steroid hormone biosynthesis, Steroid degradation pathways/ steroids
Sterol	266.247	0.000666	0.014339605	C17H28O1	[M+NH4] ¹⁺	Steroids
ST 19:3:O2 (androst-5-ene-3,17-dione)†	287.2007	0.000666	0.014339605	C19H26O2	[M+H] ¹⁺	Steroid hormone biosynthesis, Steroid degradation pathways/ steroids
	304.2276				[M+NH4] ¹⁺	

ST 19:0;O2	293.2467	0.000666	0.014339605	C19H32O2	[M+H] ¹⁺	Sterol lipids
ST 19:3;O3	303.1954	0.000666	0.014339605	C19H26O3	[M+H] ¹⁺	Sterol lipids
ST 19:2;O	273.2204	0.000666	0.014339605	C19H28O1	[M+H] ¹⁺	Sterol lipids
2-Polyprenyl-6-methoxyphenol	278.2106	0.000666	0.014339605	C17H24O2	[M+NH4] ¹⁺	Ubiquinone and other terpenoid-quinone biosynthesis/ prenol lipid
CAR 10:0	338.2316	0.000666	0.014339605	C17H33N1O4	[M+Na] ¹⁺	Acyl carnitine

(*) is an m/z with more than one possible database match, (†) is a database hit detected as multiple adducts

Table S9. Putatively identified metabolites and lipids in control group of M2 (Welch's *t*-test)

Compound name	m/z	P-value	P.adjust	Formula	Adduct	Pathway/Class
ST 27:3:O	383.331	0.000613	0.025006	C27H42O1	[M+H] ¹⁺	Sterol lipids/Steroid biosynthesis
TG 43:0	754.6889	0.000429	0.018824	C46H88O6	[M+NH4] ¹⁺	Glycerolipids (Triacylglycerols)
TG 44:0	768.7058	0.000304	0.014298	C47H90O6	[M+NH4] ¹⁺	Glycerolipids (Triacylglycerols)
TG 46:0	796.7357	0.001181	0.041687	C49H94O6	[M+NH4] ¹⁺	Glycerolipids (Triacylglycerols)
TG 47:0	810.7521	0.003086	0.080534	C50H96O6	[M+NH4] ¹⁺	Glycerolipids (Triacylglycerols)
TG 49:2	834.7522	0.003198	0.082676	C52H96O6	[M+NH4] ¹⁺	Glycerolipids (Triacylglycerols)
TG 50:2	848.7697	0.000436	0.019055	C53H98O6	[M+NH4] ¹⁺	Glycerolipids (Triacylglycerols)
TG 50:1	850.7843	0.003357	0.085523	C53H100O6	[M+NH4] ¹⁺	Glycerolipids (Triacylglycerols)
TG 51:2	862.786	0.001773	0.055668	C54H100O6	[M+NH4] ¹⁺	Glycerolipids (Triacylglycerols)

Table S10. Putatively identified metabolites and lipids in control group of M2 (Wilcoxon rank-sum test)

Compound name	m/z	P-value	P-adjust	Formula	Adduct	Pathway/Class
4-Methylpentanal	101.0963	0.000666	0.0066047	C6H12O1	[M+H] ¹⁺	Steroid hormone biosynthesis
trans-1,2-Dihydrobenzene-1,2-diol	113.06	0.000666	0.0066047	C6H8O2	[M+H] ¹⁺	Organooxygen compounds
1-Pyrroline-5-carboxylic acid	114.0553*	0.000666	0.0066047	C5H7N1O2	[M+H] ¹⁺	Arginine and proline metabolism, Alanine, aspartate and glutamate metabolism
1-Pyrroline-2-carboxylic acid						Arginine and proline metabolism
FA 6:1	115.0756	0.000666	0.0066047	C6H10O2	[M+H] ¹⁺	Fatty acyl
FA 5:1;O (3-methyl-2-oxo-butanoic acid)	117.0548	0.000666	0.0066047	C5H8O3	[M+H] ¹⁺	Fatty acyl/Valine, leucine and isoleucine degradation
FA 6:0 (isocaproic acid)	117.0911	0.000666	0.0066047	C6H12O2	[M+H] ¹⁺	Fatty acyl
FA 5:0;O	119.0704	0.000666	0.0066047	C5H10O3	[M+H] ¹⁺	Fatty acyl
FA 7:1	129.0911	0.000666	0.0066047	C7H12O2	[M+H] ¹⁺	Fatty acyl
FA 6:1;O	131.0703	0.000666	0.0066047	C6H10O3	[M+H] ¹⁺	Fatty acyl
m-Methylacetophenone	135.0804	0.000666	0.0066047	C9H10O1	[M+H] ¹⁺	Alkyl-phenylketones
3-Nonen-5-one	141.1273*	0.000666	0.0066047	C9H16O1	[M+H] ¹⁺	Enones
(3E)-2,3,4-trimethylhex-3-enal						Organooxygen compounds
Ethyl 2-hydroxyisovalerate	147.1014*	0.000666	0.0066047	C7H14O3	[M+H] ¹⁺	Fatty acyl
3-hydroxyheptanoic acid						Hydroxy acids
FA 8:2;O	157.0857	0.000666	0.0066047	C8H12O3	[M+H] ¹⁺	Fatty acyl
FA 8:1;O	159.1013	0.000666	0.0066047	C8H14O3	[M+H] ¹⁺	Fatty acyl
FA 7:1;O2	161.0805	0.000666	0.0066047	C7H12O4	[M+H] ¹⁺	Fatty acyl
FA 8:0;O	161.1169	0.000666	0.0066047	C8H16O3	[M+H] ¹⁺	Fatty acyl
FA 8:2;O2	173.0807	0.000666	0.0066047	C8H12O4	[M+H] ¹⁺	Fatty acyl
FA 10:0	173.1535	0.000666	0.0066047	C10H20O2	[M+H] ¹⁺	Fatty acyl
2,4-Dimethyladipic acid	175.0964*	0.000666	0.0066047	C8H14O4	[M+H] ¹⁺	Fatty acyl
3-Methylpimelic acid						
Isoamyl 2-furoate	183.101	0.000666	0.0066047	C10H14O3	[M+H] ¹⁺	Furans
FA 12:0;O	217.1791	0.000666	0.0066047	C12H24O3	[M+H] ¹⁺	Fatty acyl

Farnesol	223.2054	0.000666	0.0066047	C15H26O1	[M+H] ¹⁺	Prenol lipid/intermediate in the isoprenoid/cholesterol biosynthetic pathway
Glutaconylcarnitine	291.1561	0.000666	0.0066047	C12H19N1O6	[M+NH4] ¹⁺	Acyl carnitine
LPC O-18:0	510.3917	0.000666	0.0066047	C26H56N1O6P1	[M+H] ¹⁺	Glycerophospholipids/Ether lipid metabolism
PE 36:1	768.5513*	0.012654	0.0881914	C41H80N1O8P1	[M+Na] ¹⁺	Glycerophospholipid
PC 35:4				C43H78N1O8P1	[M+H] ¹⁺	Glycerophospholipid/Glycerophospholipid metabolism, Linoleic acid metabolism, alpha-Linolenic acid metabolism, Arachidonic acid metabolism
PE 38:4				C43H78N1O8P1	[M+H] ¹⁺	Glycerophospholipid/glycerophospholipid metabolism
PA 40:5				C43H75O8P1	[M+NH4] ¹⁺	Glycerophospholipid
PE O-38:4	776.5547	0.004662	0.039055	C43H80N1O7P1	[M+Na] ¹⁺	Glycerophospholipid
SM 40:1;O2	787.6657	0.000666	0.0066047	C45H91N2O6P1	[M+H] ¹⁺	Sphingolipids/Sphingolipid metabolism
PC 35:3	792.55*	0.007992	0.0609945	C43H80N1O8P1	[M+Na] ¹⁺	Glycerophospholipid
PE 38:3						
PC 37:6				C45H78N1O8P1	[M+H] ¹⁺	
PE 40:6						
PA 42:7				C45H75O8P1	[M+NH4] ¹⁺	

(*) is an m/z with more than one possible database match

Table S11. Putatively identified metabolites and lipids in Ebola VLP treatment group of M2 (Welch's *t*-test)

Compound name	m/z	P-value	P.adjust	Formula	Adduct	Pathway/Class
ST 18:3:O2(Estradiol)	273.1843	1.16184E-05	0.00105843	C18H24O2	[M+H]1+	Steroid hormone biosynthesis
5-Hydroxyindoleacetyl-glycine	287.0415	1.03816E-05	0.0009686	C12H12N2O4	[M+K]1+	Tryptophan metabolism
ST 19:4:O3†	301.18	0.00033297	0.01542121	C19H24O3	[M+H]1+	Steroid hormone biosynthesis/sterol lipids
	323.1618	2.8047E-05	0.00193454	C19H24O3	[M+Na]1+	
FA 20:4;O	338.2681	3.76837E-06	0.00054919	C20H32O3	[M+NH4]1+	Arachidonic acid metabolism/ fatty acyl (eicosanoid)
Dityrosine	361.1391	0.000797088	0.03039643	C18H20N2O6	[M+H]1+	Biomarker to several diseases/ associated with acute inflammation
FA 20:3;O (15(S)-Hydroxyeicosatrienoic acid)	361.213	0.004208524	0.09828202	C20H34O3	[M+K]1+	Modulates arachidonic acid metabolism and tumorigenesis/ fatty acyl (eicosanoid)
DG 16:0	362.29	9.34923E-06	0.00089832	C19H36O5	[M+NH4]1+	Glycerolipids (Diradylglycerols)
FA 22:0;O	374.3616	0.00413101	0.09717925	C22H44O3	[M+NH4]1+	Fatty acyl
LPC 20:4 (2-Lysolecithin)	561.3636	0.000976419	0.03578287	C28H50N1O7P1	[M+NH4]1+	Glycerophospholipid metabolism/ Glycerophospholipids
LPI 20:4	638.3289	0.004060904	0.09670559	C29H49O12P1	[M+NH4]1+	Glycerophospholipids
FA 20:0;O (Thromboxane)	314.341	0.000325363	0.01510513	C20H40O1	[M+NH4]1+	Arachidonic acid metabolism/fatty acyl (eicosanoids)
FA 22:0 (Behenic acid)	358.3663	0.000613449	0.02500635	C22H44O2	[M+NH4]1+	Biosynthesis of unsaturated fatty acids/ fatty acyl
Docosanamide	362.3391	0.003776159	0.09264222	C22H45N1O1	[M+Na]1+	Fatty amide

(†) is a database hit detected as multiple adducts

Table S12. Putatively identified metabolites and lipids in Ebola VLP treatment group of M2 (Wilcoxon rank-sum test)

Compound name	m/z	P-value	P.adjust	Formula	Adduct	Pathway/Class
1,2-Dihydronaphthalene-1,2-diol	180.1014	0.000666	0.0066047	C10H10O2	[M+NH4] ¹⁺	1,2-Dihydronaphthalene-1,2-diol is a primary metabolite. Primary metabolites are metabolically or physiologically essential metabolites. They are directly involved in an organism's growth, development or reproduction
20-HETE ethanolamide	364.284*	0.000666	0.0066047	C22H37N1O3	[M+H] ¹⁺	N-acyl ethanolamine
Leukotriene B4 dimethylamide						A derivative of Leukotriene B4 (which is involved in the Arachidonic acid metabolism pathway)/ fatty acyl (eicosanoid)
CAR 4:0	232.1539	0.000666	0.0066047	C11H21N1O4	[M+H] ¹⁺	Acyl carnitine
CAR 7:0	274.2004	0.000666	0.0066047	C14H27N1O4	[M+H] ¹⁺	Acyl carnitine
CAR (Heptanoyl carnitine)						
CAR 6:0	276.1796	0.000666	0.0066047	C13H25N1O5	[M+H] ¹⁺	Acyl carnitine
CAR 5:0	262.1649	0.000666	0.0066047	C12H23N1O5	[M+H] ¹⁺	Acyl carnitine
CAR 22:5	474.3564	0.000666	0.0066047	C29H47N1O4	[M+H] ¹⁺	Acyl carnitine
FA 20:5:0	319.2253	0.000666	0.0066047	C20H30O3	[M+H] ¹⁺	Arachidonic acid metabolism/ fatty acyl (eicosanoid)
FA 20:5:0	336.2523	0.000666	0.0066047	C20H30O3	[M+NH4] ¹⁺	Arachidonic acid metabolism/ fatty acyl (eicosanoid)
N-palmitoyl glycine				C18H35N1O3	[M+Na] ¹⁺	Fatty amide
Tetranor 12-HETE	267.195	0.000666	0.0066047	C16H26O3	[M+H] ¹⁺	Arachidonic acid metabolism/ fatty acyl (eicosanoid)(it enhances tumor cell adhesion to endothelial cells, fibronectin, and the subendothelial matrix)
L-Proline	116.0709*	0.000666	0.0066047	C5H9N1O2	[M+H] ¹⁺	Arginine and proline metabolism
Acetamidopropanal						Associated with urea cycle and metabolism of arginine, proline, glutamate, aspartate and asparagine.

FA 20:5 (EPA)	303.2318	0.000666	0.0066047	C20H30O2	[M+H] ¹⁺	Biosynthesis of unsaturated fatty acids/ fatty acyl
3-Cyclohexene-1-carboxaldehyde, 1,3,4-trimethyl	153.127*	0.000666	0.0066047	C10H16O1	[M+H] ¹⁺	Cycloalkanes
4-(1-Methylethyl)-1-cyclohexene-4-carboxaldehyde						
FA 18:1	283.2631	0.000666	0.0066047	C18H34O2	[M+H] ¹⁺	Fatty acyl
FA 20:2	309.2781	0.000666	0.0066047	C20H36O2	[M+H] ¹⁺	Fatty acyl
10-Nitrolinoleic acid	343.2588	0.000666	0.0066047	C18H31N1O4	[M+NH4] ¹⁺	Fatty acyl
FA 10:1;O3	236.1487	0.000666	0.0066047	C10H18O5	[M+NH4] ¹⁺	Fatty acyl
FA 14:1	244.2267	0.000666	0.0066047	C14H26O2	[M+NH4] ¹⁺	Fatty acyl
FA 17:1	286.274	0.000666	0.0066047	C17H32O2	[M+NH4] ¹⁺	Fatty acyl
FA 19:3;O	326.2688	0.000666	0.0066047	C19H32O3	[M+NH4] ¹⁺	Fatty acyl
FA 14:1	244.2267	0.000666	0.0066047	C14H26O2	[M+NH4] ¹⁺	Fatty acyl
FA 10:2;O2	201.112	0.000666	0.0066047	C10H16O4	[M+H] ¹⁺	Fatty acyl (Decenedioic acid)
MG 10:0	247.1903	0.000666	0.0066047	C13H26O4	[M+H] ¹⁺	Glycerolipids (Monoradylglycerols)
LPA 22:0	526.3527	0.000666	0.0066047	C25H49O8P1	[M+NH4] ¹⁺	Glycerophospholipids
FA 18:2 (linoleic acid)	281.2477	0.000666	0.0066047	C18H32O2	[M+H] ¹⁺	Linoleic acid metabolism, Biosynthesis of unsaturated fatty acids
N-Methylphenylethanolamine	169.1329	0.002664	0.0239999	C9H13N1O1	[M+NH4] ¹⁺	N-Methylphenylethanolamine is a secondary metabolite. Secondary metabolites are metabolically or physiologically non-essential metabolites that may serve a role as defense or signalling molecules
Cholesterol glucuronide	585.3749	0.000666	0.0066047	C33H54O7	[M+Na] ¹⁺	Pentose and glucuronate interconversions
Deoxyribose	135.0651*	0.000666	0.0066047	C5H10O4	[M+H] ¹⁺	Pentose phosphate pathway
FA 5:0;O2						Valine, leucine and isoleucine biosynthesis, Pantothenate and CoA biosynthesis/fatty acyl

13 ¹ -Carboxy-gamma-tocopherol	469.3277	0.000666	0.0066047	C28H46O4	[M+Na] ¹⁺	Prenol lipid
Dehydroabietic acid	301.2159*	0.000666	0.0066047	C20H28O2	[M+H] ¹⁺	Prenol lipids
Retinoic Acid						Retinol metabolism/ prenenol lipids
ST 24:1;O4	410.3252	0.000666	0.0066047	C24H40O4	[M+NH4] ¹⁺	Primary and Secondary bile acid biosynthesis/ terol lipids
ST 19:2;O2	289.2159	0.000666	0.0066047	C19H28O2	[M+H] ¹⁺	Steroid hormone biosynthesis/ sterol lipids
ST 19:1;O2†	291.2313	0.000666	0.0066047	C19H30O2	[M+H] ¹⁺	Steroid hormone biosynthesis/ sterol lipids
	308.258				[M+NH4] ¹⁺	
ST (Androstenedione)	287.2007	0.000666	0.0066047	C19H26O2	[M+H] ¹⁺	Steroid hormone biosynthesis/ sterol lipids
ST 19:2;O3 (17beta,19-dihydroxyandrost-4-en-3-one)	305.2109	0.000666	0.0066047	C19H28O3	[M+H] ¹⁺	Steroid hormone biosynthesis/ sterol lipids
ST 19:4;O3	318.2052	0.000666	0.0066047	C19H24O3	[M+NH4] ¹⁺	Steroid hormone biosynthesis/ sterol lipids
ST 19:0;O2†	293.2467	0.000666	0.0066047	C19H32O2	[M+H] ¹⁺	Steroid hormone biosynthesis/ sterol lipids
	310.2735				[M+NH4] ¹⁺	
ST 19:2;O	273.2204	0.000666	0.0066047	C19H28O1	[M+H] ¹⁺	Sterol lipid
ST 19:1;O3	307.2264	0.000666	0.0066047	C19H30O3	[M+H] ¹⁺	Sterol lipids
	324.2532				[M+NH4] ¹⁺	
Tetrahydropteridine	159.0649*	0.000666	0.0066047	C6H8N4	[M+Na] ¹⁺	Pteridines
Succinylacetone					[M+H] ¹⁺	Succinylacetone can act as an acidogen, an oncometabolite, and a metabotoxin
Isopropylmaleic acid				C7H10O4		Valine, leucine and isoleucine biosynthesis

(*) is an m/z with more than one possible database match, (†) is a database hit detected as multiple adducts

